Supersymmetric Regularization, Two-Loop QCD Amplitudes and Coupling Shifts

Z. Bern[⋆]

Department of Physics and Astronomy
UCLA, Los Angeles, CA 90095-1547

A. De Freitas[⋆]

Department of Physics and Astronomy
UCLA, Los Angeles, CA 90095-1547

L. Dixon[†]

Stanford Linear Accelerator Center
Stanford University
Stanford, CA 94309

and

H.L. Wong[⋆]

Department of Physics and Astronomy
UCLA, Los Angeles, CA 90095-1547

Abstract

We present a definition of the four-dimensional helicity (FDH) regularization scheme valid for two or more loops. This scheme was previously defined and utilized at one loop. It amounts to a variation on the standard 't Hooft-Veltman scheme and is designed to be compatible with the use of helicity states for "observed" particles. It is similar to dimensional reduction in that it maintains an equal number of bosonic and fermionic states, as required for preserving supersymmetry. Supersymmetry Ward identities relate different helicity amplitudes in supersymmetric theories. As a check that the FDH scheme preserves supersymmetry, at least through two loops, we explicitly verify a number of these identities for gluon-gluon scattering ($gg \to gg$) in supersymmetric QCD. These results also cross-check recent non-trivial two-loop calculations in ordinary QCD. Finally, we compute the two-loop shift between the FDH coupling and the standard $\overline{\text{MS}}$ coupling, α_s. The FDH shift is identical to the one for dimensional reduction. The two-loop coupling shifts are then used to obtain the three-loop QCD β function in the FDH and dimensional reduction schemes.

Submitted to Physical Review D

1   Introduction

It is of great utility to regularize the divergences of quantum field theory in a way that manifestly preserves the symmetries of the theory. The most widely utilized technique for preserving gauge symmetry is dimensional regularization, which can simultaneously handle the ultraviolet and infrared divergences of massless gauge theory. There are actually several common variants of dimensional regularization, differing in their treatment of the Lorentz vector indices associated with gauge particles. The different variants have advantages and disadvantages, depending on the application. The conventional dimensional regularization scheme (CDR) [1] is conceptually the simplest and most widely used variant. In this scheme one uniformly continues all momenta and vector polarizations to $D = 4 - 2\epsilon$ dimensions. The 't Hooft-Veltman (HV) scheme [2] is closely related, differing only in the treatment of "observed" states, which remain in four dimensions. The HV scheme is especially convenient for computing helicity amplitudes — as has proven very useful in QCD calculations [3, 4, 5, 6] — because only the amplitudes with the four-dimensional helicity values ± 1 (or 0, for massive vector bosons) have to be evaluated. For supersymmetric theories, the most commonly used regularization scheme is Siegel's dimensional reduction (DR) scheme [7], since it preserves supersymmetry. This scheme has also found use in certain non-supersymmetric calculations [8, 9]. Other useful schemes for supersymmetric theories include the holomorphic and NSVZ schemes [10].

Another scheme that has been used at one loop is the four-dimensional helicity (FDH) scheme[5]. The FDH scheme seeks to combine the natural use of helicity states (as in the HV scheme) with the preservation of supersymmetry. It is similar to the DR scheme in maintaining the number of physical states at their four-dimensional values. In the FDH scheme, however, the algebraic rules are defined with the notion that $D > 4$, but with an analytic continuation to bring the number of physical states back to their $D = 4$ values. This may be contrasted with the DR scheme, where one takes $D < 4$, viewed as a dimensional compactification. The distinction between $D < 4$ and $D > 4$ is relevant only when an explicit basis of external states is required for a calculation; inside the loops in either case all indices on fields are treated as four-dimensional. At one loop, the relationship between the FDH and DR schemes has been previously discussed in ref. [11].

Preserving supersymmetry is useful even for higher order calculations in QCD. Although QCD itself is not a supersymmetric theory, one can slightly modify QCD by altering the color representations and multiplicities so that it becomes supersymmetric. The amplitudes in such a theory are closely related to those in QCD, yet they must satisfy non-trivial supersymmetry Ward identities [12, 13], as long as the regulator preserves supersymmetry. These identities can therefore provide an independent means for checking a non-trivial QCD calculation. The supersymmetry identities on scattering amplitudes are phrased in terms of the helicity basis; thus the FDH scheme is ideal for using supersymmetry in this way. Of course one would also want to have available a simple way to convert amplitudes computed in the standard variants of dimensional regularization, such as the 't Hooft-Veltman (HV) or conventional dimensional regularization (CDR) schemes, into those computed in the FDH scheme, or vice-versa.

Though we do not have a proof that the FDH scheme preserves supersymmetry to all orders of perturbation theory, it inherently maintains the number of physical states at their four-dimensional

values. Moreover, from explicit calculations the scheme is known to preserve supersymmetry at one loop [11]. In this paper we shall explicitly verify its preservation at two loops, by checking various supersymmetry identities involving $gg \to gg$ helicity amplitudes.

The issue of higher-loop regularization is timely in light of the recent substantial progress in the calculation of two-loop scattering amplitudes. Until recently, no such amplitudes depending on more than a single kinematic variable were known. Now several such computations have appeared. The first of these were gluon-gluon scattering amplitudes in the special cases of maximal ($N = 4$) supersymmetry [14], and for a particular gluon helicity configuration in pure Yang-Mills theory [15]. Subsequently, complete calculations have been performed for Bhabha scattering [16], general $2 \to 2$ parton scattering in QCD [17, 18, 19], the di-photon background to Higgs production at the LHC [20], and light-by-light scattering [21].

Important technical breakthroughs, which allowed the more general calculations to proceed, included the reduction of the two loop momentum integrals appearing in the all-massless $2 \to 2$ processes to a set of master integrals, and the evaluation of those master integrals as a Laurent series in ϵ [22, 23, 24, 25, 26, 27]. Even more recently, the corresponding integrals where one of the four external legs is massive have been evaluated [28], enabling the computation of the two-loop amplitudes for e^+e^- annihilation into three partons [29].

In our explicit verification of supersymmetry identities, we investigate the $gg \to gg$ helicity amplitudes

$$\mathcal{A}_4(1_g^{\pm}, 2_g^+, 3_g^+, 4_g^+), \tag{1.1}$$

where the subscript labels the particle species (g for gluon), and the superscript denotes the sign of the helicity. We use an "all-outgoing" helicity convention: if a given leg is incoming, then the actual helicity is the opposite of the superscript label. We study the helicity amplitudes (1.1) because they are relatively simple (for two-loop amplitudes), and because supersymmetry is especially constraining. For both the $++++$ and $-+++$ helicity configurations, we have computed all the gluon and fermion loop contributions that appear in QCD. For the $++++$ configuration, we have also included scalars with both gauge and Yukawa interactions, to allow for a more extensive test of supersymmetry identities.

It is important to be able to convert helicity amplitudes computed in the FDH scheme to the more standard CDR and HV schemes, and vice versa. A given dimensional regularization scheme has implications for regularization of both ultraviolet and infrared singularities. Both the ultraviolet and infrared aspects of scheme conversion have been extensively discussed at one loop [5, 11, 30], and to some degree at two loops [19]. The infrared aspects are not yet understood for arbitrary processes, as only the $gg \to gg$ process was studied in ref. [19]. Conversion from one scheme to another in the ultraviolet, though, is a process-independent procedure. It just amounts to relating the two different renormalized couplings implied by the two schemes, to a sufficiently high accuracy in perturbation theory. The FDH and $\overline{\text{DR}}$ schemes behave the same in the ultraviolet; their couplings are identical. The relation between the $\overline{\text{DR}}$ (or FDH) and $\overline{\text{MS}}$ versions of α_s in QCD has been known to one-loop accuracy for some time [8, 31, 32, 11]. Here we extend the relation to two-loop accuracy.

The first two coefficients of the QCD β function are scheme-independent (for analytic redefinitions

of the coupling), but the three-loop coefficient, b_2, depends on the scheme. However, knowing the value of b_2 in the $\overline{\text{MS}}$ scheme [33], and the two-loop relation between couplings, we can easily obtain the value of b_2 in the $\overline{\text{DR}}$ (or FDH) scheme.

This paper is organized as follows. In sect. 2 we review the supersymmetry Ward identities. We then present the rules for the FDH scheme in sect. 3. In performing the explicit two-loop calculations, we did not use Feynman diagrams directly. Instead we computed (generalized) unitarity cuts of the amplitudes in all channels and to all order in ϵ. Then the amplitude was reconstructed from the cuts. This cutting method is described in sect. 4. In sect. 5 we perform a color decomposition of the two-loop amplitude, into color structures multiplied by "primitive" functions which have been stripped of color. This decomposition makes it convenient to obtain either QCD or supersymmetric amplitudes. The primitive amplitudes used in our explicit check of the two-loop supersymmetry Ward identities are presented in sect. 6. We verify the identities in sect. 7. In sect. 8 we discuss ultraviolet renormalization, the two-loop shifts in the couplings and amplitudes, and their implications for the three-loop β function.

2 Supersymmetry Ward identities

Helicity amplitudes in supersymmetric theories are subject to a set of stringent conditions imposed by the super-algebra: the S-matrix supersymmetry Ward identities (SWI) [12, 13]. These identities allow us to distill the information contained in the supersymmetry algebra and apply it directly to on-shell S-matrix elements. They hold in any supersymmetric theory. They also lead to relations among different components of amplitudes in any non-supersymmetric theory, such as QCD, for which a re-adjustment of color representations and/or multiplicities makes the theory supersymmetric. At tree level and at one loop, supersymmetry Ward identities have been applied to QCD, either as checks or as computational aids [13, 34, 11, 35, 6]. As we discuss in this paper, the same ideas can be applied at two loops.

2.1 Derivation

The derivation of the supersymmetry Ward identities from the super-algebra has been discussed in the literature in a number of articles and reviews [12, 4], so we describe it only briefly. Since we are interested in applications to non-supersymmetric theories we phrase the supersymmetry identities in terms of the component fields. The $N = 1$ super-algebra describing the action of the super-charge on the component gluon field g and gluino field λ comprising the vector supermultiplet is

$$[Q(p), g^{\pm}(k)] = \mp \Gamma^{\pm}(k, p)\, \lambda^{\pm}(k)\,, \qquad\qquad [Q(p), \lambda^{\pm}(k)] = \mp \Gamma^{\mp}(k, p)\, g^{\pm}(k)\,, \qquad (2.1)$$

where k is the light-like momentum carried by the field, $Q(p)$ is the super-charge contracted with a spinor for the (arbitrary) light-like vector p, and

$$\Gamma^{+}(k, p) = \bar{\theta}\, [p\, k]\,, \qquad\qquad \Gamma^{-}(k, p) = \theta\, \langle p\, k \rangle\,.$$

Because Γ^{-} is proportional to a Grassmann variable θ and Γ^{+} is proportional to $\bar{\theta}$, the coefficients Γ^{+} and Γ^{-} in a supersymmetry Ward identity are independent. We use the notation $\langle k_i^{-} | k_j^{+} \rangle = \langle i\, j \rangle$

and $\langle k_i^+ | k_j^- \rangle = [i\,j]$, where $|k_i^\pm\rangle$ are massless Weyl spinors with momentum k_i, labeled with the sign of the helicity and normalized by $\langle i\,j\rangle [j\,i] = s_{ij} = 2k_i \cdot k_j$. Note that $\langle i\,i\rangle = [i\,i] = 0$.

Since the super-charge $Q(p)$ annihilates the vacuum, one can construct a typical $N = 1$ supersymmetry Ward identity in the following way:

$$
\begin{aligned}
0 = \langle 0 | [Q, g_1^\pm g_2^+ \lambda_3^+ g_4^+] | 0 \rangle = {} & \mp \Gamma^\pm(k_1, p) \mathcal{A}_4^{\mathrm{SUSY}}(1_\lambda^\pm, 2_g^+, 3_\lambda^+, 4_g^+) - \Gamma^+(k_2, p) \mathcal{A}_4^{\mathrm{SUSY}}(1_g^\pm, 2_\lambda^+, 3_\lambda^+, 4_g^+) \\
& - \Gamma^-(k_3, p) \mathcal{A}_4^{\mathrm{SUSY}}(1_g^\pm, 2_g^+, 3_g^+, 4_g^+) + \Gamma^+(k_4, p) \mathcal{A}_4^{\mathrm{SUSY}}(1_g^\pm, 2_g^+, 3_\lambda^+, 4_\lambda^+),
\end{aligned}
\tag{2.2}
$$

where $\mathcal{A}_4^{\mathrm{SUSY}}$ is a four-point amplitude in a supersymmetric theory, the integers refer to the leg labels, and the subscripts g and λ to the particle species of the specified leg. Since the coefficients of Γ^+ and Γ^- are independent, the sum of the terms with Γ^- prefactors must vanish independently. (The Γ^+ terms in eq. (2.2) also vanish using gluino helicity conservation.) By choosing $p = k_1$ we obtain the identity,

$$
\mathcal{A}_4^{\mathrm{SUSY}}(1_g^\pm, 2_g^+, 3_g^+, 4_g^+) = 0,
\tag{2.3}
$$

which is the main SWI that we will investigate at two loops in this paper.

Using the super-algebra, one may systematically derive other identities. The nonvanishing amplitudes with external gluons only are related to amplitudes containing external gluinos, e.g.,

$$
\begin{aligned}
\mathcal{A}_4^{\mathrm{SUSY}}(1_g^-, 2_\lambda^-, 3_\lambda^+, 4_g^+) &= \frac{\langle 1\,3\rangle}{\langle 1\,2\rangle}\, \mathcal{A}_4^{\mathrm{SUSY}}(1_g^-, 2_g^-, 3_g^+, 4_g^+), \\
\mathcal{A}_4^{\mathrm{SUSY}}(1_\lambda^-, 2_\lambda^+, 3_\lambda^-, 4_\lambda^+) &= \frac{\langle 2\,4\rangle}{\langle 1\,3\rangle}\, \mathcal{A}_4^{\mathrm{SUSY}}(1_g^-, 2_g^+, 3_g^-, 4_g^+).
\end{aligned}
\tag{2.4}
$$

The amplitudes on the right-hand side of eq. (2.4) have recently been computed at two loops [19]. The amplitudes on the left-hand side are related to the QCD amplitudes for $q\bar{q} \to gg$, $qg \to qg$, $q\bar{q} \to q\bar{q}$, and $qq \to qq$, but these amplitudes have not yet been computed at two loops in the helicity formalism,[1] and we shall not do so here.

2.2 Lagrangian

To allow us to separate out different supersymmetric combinations of amplitudes, we consider $N = 1$ supersymmetric $SU(N_c)$ gauge theory with two different types of matter content:

1. n_f identical chiral matter multiplets Q_i, $i = 1, \ldots, n_f$, transforming in the **fundamental** N_c representation of the gauge group, and their $\bar{N}_c$ partners $\tilde{Q}_i$, with vanishing superpotential, $W = 0$.

2. A single chiral matter multiplet $\Phi \equiv \Phi^a T^a$ transforming in the **adjoint** representation, with superpotential $W = \frac{1}{3} g\xi \operatorname{Tr}\Phi^3$, where Tr is an $SU(N_c)$ trace. For convenience, we write the Yukawa coupling as $g\xi$, and take ξ to be independent of the gauge coupling g.

---

[1] They have been computed, and the SWI have been verified, at one loop [11]. At two loops, the interference with the tree amplitude, summed over all external colors and helicities, has been computed [17], but the conversion to a supersymmetric amplitude has not yet been performed.

Our $SU(N_c)$ generators are normalized by $\text{Tr}(T^a T^b) = \delta^{ab}$. Because of the gauge symmetry, gluons couple to all other particles via the standard gauge theory interaction for fermions or scalars, with gauge coupling g. The couplings of gluinos or matter fermions may be conveniently extracted from the component expansion of the interaction Lagrangian [36].

The interaction terms in the case of fundamental matter are

$$
\begin{aligned}
\mathcal{L}_g^{\text{fund}} = {} & ig \sum_{i=1}^{n_f} \left((A_i^* T^a \psi_i - \tilde{\psi}_i T^a \tilde{A}_i^*) \lambda^a - \bar{\lambda}^a (A_i T^a \bar{\psi}_i - \bar{\tilde{\psi}}_i T^a \tilde{A}_i) \right) \\
& - \frac{g^2}{4} \left(\sum_{i=1}^{n_f} (A_i^* T^a A_i - \tilde{A}_i T^a \tilde{A}_i^*) \right)^2 ,
\end{aligned}
\tag{2.5}
$$

following the notation of Wess and Bagger [37], chapter 7. Here $\lambda \equiv \lambda^a T^a$ is the gluino; A_i and ψ_i are, respectively, the scalar and fermionic components of Q_i, while $\tilde{A}_i$ and $\tilde{\psi}_i$ are the corresponding components of $\tilde{Q}_i$.

In the case of adjoint matter, the interaction terms proportional to the gauge coupling are,

$$
\begin{aligned}
\mathcal{L}_g^{\text{adjoint}} &= -ig \, \text{Tr}([A^*, \psi] \lambda) + ig \, \text{Tr}([A, \bar{\psi}] \bar{\lambda}) - \frac{g^2}{4} \sum_a \text{Tr}([A, A^*] T^a)^2 \\
&= -ig \, \text{Tr}([A^*, \psi] \lambda) + ig \, \text{Tr}([A, \bar{\psi}] \bar{\lambda}) - \frac{g^2}{2} \text{Tr}(AA^* AA^* - A^2 A^{*2}) .
\end{aligned}
\tag{2.6}
$$

The terms arising from the superpotential W are

$$
\begin{aligned}
\mathcal{L}_\xi^{\text{adjoint}} &= -g\xi \, \text{Tr} \psi\psi A - g\xi^* \, \text{Tr} \bar{\psi}\bar{\psi} A^* - g^2 |\xi|^2 \sum_a \text{Tr}(A^2 T^a) \, \text{Tr}(A^{*2} T^a) \\
&= -g\xi \, \text{Tr} \psi\psi A - g\xi^* \, \text{Tr} \bar{\psi}\bar{\psi} A^* - g^2 |\xi|^2 \left[\text{Tr} A^2 A^{*2} - \frac{1}{N_c} \text{Tr} A^2 \, \text{Tr} A^{*2} \right] .
\end{aligned}
\tag{2.7}
$$

2.3 Amplitude decomposition by particle content

Supersymmetry can be exploited in non-supersymmetric theories such as QCD [13, 4, 6] by observing that appropriate linear combinations of quantities occurring in QCD amplitudes are in fact supersymmetric. As an especially simple example, at tree level an n-gluon amplitude is automatically supersymmetric [13]. Since the fermions do not appear in intermediate states, the fermions in the theory might as well be in the adjoint representation, *i.e.*, the theory might as well be pure $N = 1$ super-Yang-Mills theory. Thus, by virtue of eq. (2.3), the four-gluon tree amplitude in QCD satisfies,

$$
\mathcal{A}_4^{\text{QCD tree}}(1_g^\pm, 2_g^+, 3_g^+, 4_g^+) = 0 .
\tag{2.8}
$$

At loop level the application of supersymmetry in QCD is clearly more intricate, because all particles in the theory can circulate in the loops. Nevertheless, one can still use supersymmetry to relate different contributions.

At one loop, the four-gluon amplitude in supersymmetric QCD with n_f matter multiplets — case 1 in sect. 2.2 — has the structure,

$$
\mathcal{A}_4^{N=1} = \mathcal{A}_4^{\text{vector}} + n_f \mathcal{A}_4^{\text{matter}} ,
\tag{2.9}
$$

where the contribution $\mathcal{A}_4^{\text{vector}}$ is that of a vector multiplet consisting of a gluon and gluino, and $\mathcal{A}_4^{\text{matter}}$ is that of a matter multiplet consisting of a quark and squark. Identities may be obtained from each term in this decomposition. For example, by setting $n_f = 0$ in eq. (2.9), corresponding to pure $N = 1$ super-Yang-Mills theory, from the SWI (2.3) we have,

$$\mathcal{A}_4^{\text{gluon loop}}(1_g^\pm, 2_g^+, 3_g^+, 4_g^+) = -\mathcal{A}_4^{\text{gluino loop}}(1_g^\pm, 2_g^+, 3_g^+, 4_g^+)\,, \tag{2.10}$$

which relates the gluon loop contribution depicted in fig. 1(a) to the fermion loop contribution depicted in fig. 1(b). To apply this identity to QCD, one uses group theory to relate the contribution of an adjoint representation fermion (gluino) in the loop to that of a fundamental representation fermion (quark), as we shall describe further in section 5.1.

Similarly, by considering the contribution from an $N = 1$ matter multiplet, consisting of a fermion and a scalar transforming in the same representation of the gauge group, *i.e.*, the n_f-dependent term in eq. (2.9), we obtain

$$\mathcal{A}_4^{\text{scalar loop}}(1_g^\pm, 2_g^+, 3_g^+, 4_g^+) = -\mathcal{A}_4^{\text{fermion loop}}(1_g^\pm, 2_g^+, 3_g^+, 4_g^+)\,, \tag{2.11}$$

which relates the fermion loop contribution in fig. 1(b) to the scalar loop contribution in fig. 1(c). By supersymmetry, the number of physical states in the scalar loop matches that in the fermion loop. For a scalar in the adjoint representation of $SU(N_c)$, paired with a Majorana gluino (in $N = 2$ supersymmetry, say), this amounts to $2 \times (N_c^2 - 1)$ states. For a fundamental representation scalar, paired with a quark (a Dirac fermion), it amounts to $4 \times N_c$ states. (At the one-loop level, considering adjoint matter with a superpotential — case 2 in sect. 2.2 — leads to no new identities from the four-gluon amplitude.)
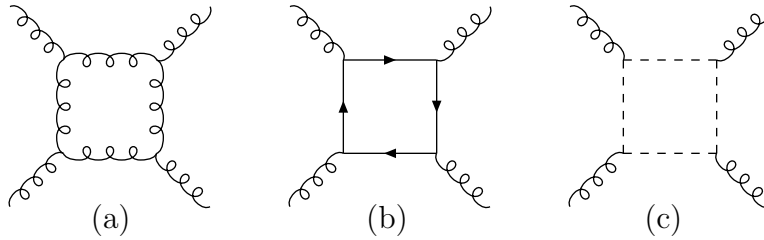

Figure 1: Sample diagrams contributing to: (a) a gluon circulating in the loop, (b) a fermion circulating in the loop, and (c) and scalar circulating in the loop.

These considerations extend to two loops. In the case of n_f matter multiplets in the fundamental representation — case 1 in sect. 2.2 — the four-gluon amplitude takes the form,

$$\mathcal{A}_4^{N=1,\,\text{fund}} = \mathcal{A}_4^{\text{vector}} + n_f \mathcal{A}_4^{\text{matter(1)}} + n_f^2 \mathcal{A}_4^{\text{matter(2)}}\,. \tag{2.12}$$

In the case of one adjoint matter multiplet with a superpotential — case 2 in sect. 2.2 — the four-gluon amplitude takes the form,

$$\mathcal{A}_4^{N=1\,\text{adj}} = \mathcal{A}_4^{\text{vector}} + \mathcal{A}_4^{\text{matter(1)}} + \mathcal{A}_4^{\text{matter(2)}} + |\xi|^2 \mathcal{A}_4^{\text{Yukawa}}\,. \tag{2.13}$$

The quantities $\mathcal{A}_4^{\text{matter}(i)}$ are "dressed" differently with color in the two cases, as will be explained in sect. 5. We have subdivided the contributions according to their dependence on the number of matter multiplets and on the couplings. Identities may be obtained from each term in the decomposition (2.12), and from the ξ-dependent term in eq. (2.13), because n_f and ξ are independent parameters. Representative diagrams contributing to each of the four independent supersymmetric components $\mathcal{A}_4^{\text{vector}}$, $\mathcal{A}_4^{\text{matter}(1)}$, $\mathcal{A}_4^{\text{matter}(2)}$ and $\mathcal{A}_4^{\text{Yukawa}}$ are depicted in figs. 2(a)–(d).
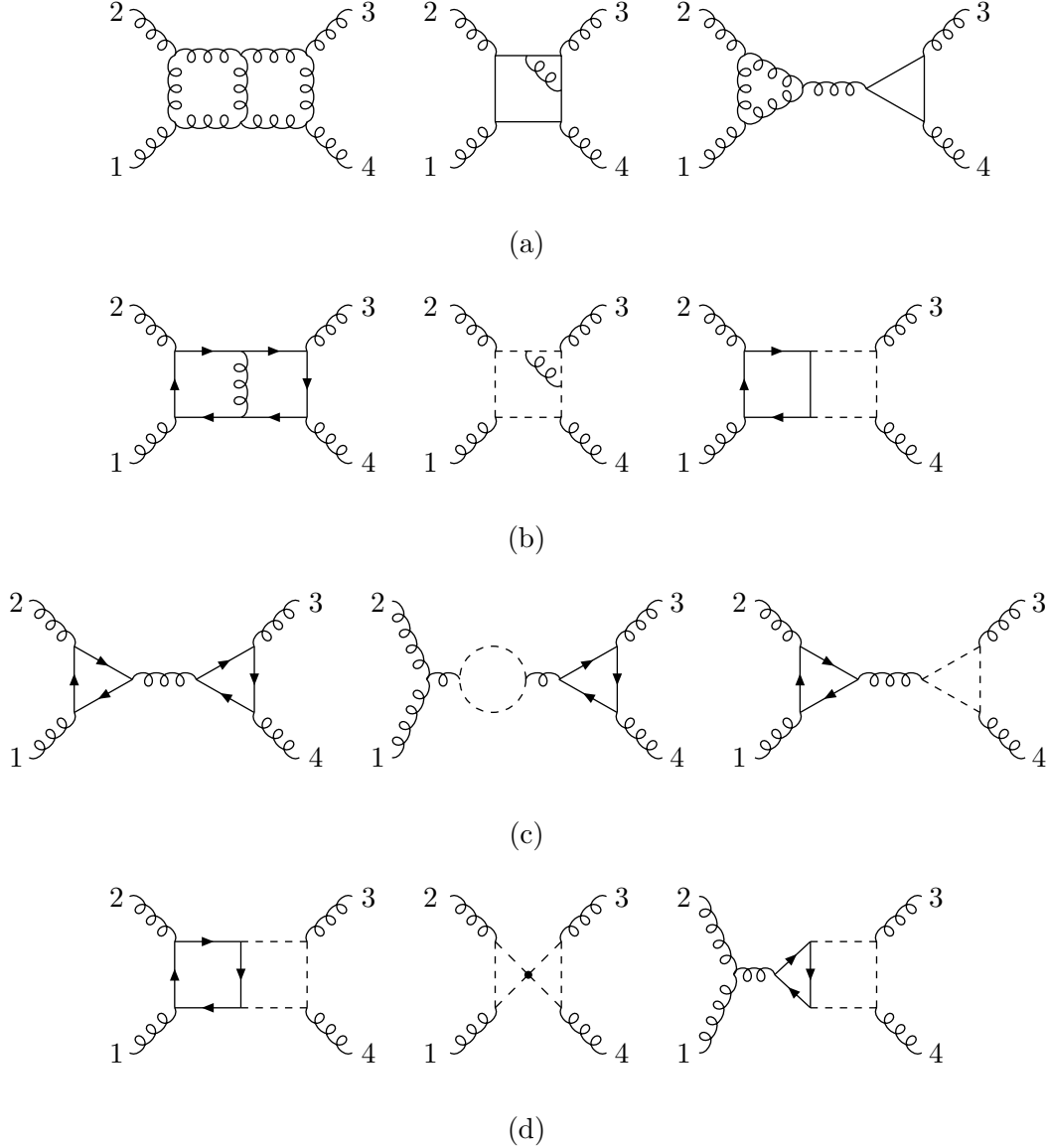

(a)

(b)

(c)

(d)

Figure 2: Representative diagrams contributing to the supersymmetric amplitudes (a) $\mathcal{A}_4^{\text{vector}}$, (b) $\mathcal{A}_4^{\text{matter}(1)}$, (c) $\mathcal{A}_4^{\text{matter}(2)}$, and (d) $\mathcal{A}_4^{\text{Yukawa}}$ in eqs. (2.12) and (2.13). The curly, solid without arrows, solid with arrows, and dotted lines represent gluons, gluinos, quarks, and scalars, respectively.

For the helicity configurations $++++$ and $-+++$, four independent identities are obtained by setting eqs. (2.12) and (2.13) to vanish using the SWI (2.3). Each such identity actually generates several equations, once the amplitudes are further decomposed according to the colors of the external

gluons. The equations stemming from $\mathcal{A}^{\text{vector}}(\pm, +, +, +) = 0$, which only involve gluons and gluinos, can be applied to QCD once one understands the group theory relations at two loops between the contribution of fundamental and adjoint representation fermions. The remaining identities have scalar particles propagating in the loops as well. A systematic discussion of all these relations, based on "primitive" or "color-stripped" amplitudes, will be presented in sections 5-7.

3   Supersymmetric regularization

For supersymmetry identities to hold directly, a necessary condition is that the regularization should not alter the number of bosonic states relative to the number of fermionic states. The conventional and 't Hooft-Veltman variants of dimensional regularization [2, 1] are incompatible with supersymmetry precisely because they alter the balance of bosonic and fermionic degrees of freedom. In the four-dimensional limit, manifest supersymmetry will not generally be recovered in these schemes due to divergences in the amplitudes. An $\mathcal{O}(\epsilon)$ discrepancy between the number of bosonic and fermion states can be multiplied by an $1/\epsilon$ singularity, leaving a supersymmetry-violating remainder even as $\epsilon \to 0$. If the only divergences are ultraviolet in nature, it is possible to repair such violations by adding suitable finite counterterms, order by order in perturbation theory (see *e.g.* ref. [32]). However, it is clearly desirable to avoid this situation if possible, particularly in theories with a large number of coupling constants. Also, we are interested in on-shell scattering amplitudes for theories with severe infrared divergences, and here local counterterms will not suffice.

3.1   Dimensional reduction scheme

The most widely used scheme for preserving supersymmetry is the dimensional reduction (DR) [7] variant of dimensional regularization.[2] The rules for dimensional reduction follow from viewing it as a compactification of a four-dimensional theory to $D < 4$. The rules for dimensional reduction are [38]:

- As in ordinary dimensional regularization, all momentum integrals are integrated over D-component momenta. Any Kronecker $\delta_\mu{}^\nu$'s resulting from the integration are D-dimensional. (This is necessary for maintaining gauge invariance.)

- All indices on the fields, and on corresponding matrices coming from the action, are treated as four-dimensional indices.

- Since $D < 4$ always, any four-dimensional Kronecker $\delta_\mu^{(4)\nu}$ contracted with a D-dimension momentum $p_\nu^{(D)}$ yields a D-dimensional momentum, $\delta_\mu^{(4)\nu} p_\nu^{(D)} = p_\mu^{(D)}$. Similarly, for any four-dimensional vector, $\varepsilon_{(4)}^\mu$, the dot product with a D-dimensional vector yields a D-dimensional dot product, $\varepsilon_{(4)}^\mu p_\mu^{(D)} = \varepsilon_{(D)}^\mu p_\mu^{(D)}$. In general, dot products of four-dimensional vectors with (-2ϵ)-dimensional ones will not vanish.

---

[2]As is customary in essentially all variants of dimensional regularization, we treat the fermions as four-dimensional by letting the Dirac trace of the identity be $\text{tr}(1) = 4$.

The first rule is necessary for preserving gauge invariance and the second for preserving super-symmetry. It is the third rule which defines the regularization as dimensional reduction. In the DR scheme a four-dimensional vector may be viewed as a combination of the $D = 4 - 2\epsilon$ vector plus a set of (-2ϵ) scalars. In non-supersymmetric theories in the DR scheme it is especially important to keep track of the distinction between the vectors and the (-2ϵ) scalars because of their differing renormalization properties. Moreover, in the non-supersymmetric case it is essential to keep evanescent couplings and operators [9].

The rule $\varepsilon_{(4)}^{\mu} p_{\mu}^{(D)} = \varepsilon_{(D)}^{\mu} p_{\mu}^{(D)}$ is also awkward to handle in the presence of explicit four-dimensional polarization vectors $\varepsilon_{(4)}^{\mu}$. Such vectors are encountered when evaluating helicity amplitudes in (for example) the spinor helicity formalism [3]. Intuitively, for $D < 4$, there are less than 2 spatial directions transverse to the gluon direction, so one cannot really perform a rotation in this transverse plane, as required to define a helicity eigenstate.

3.2 The four-dimensional helicity scheme

Motivated by the desire of having a supersymmetric scheme whose rules are more closely related to the more conventional 't Hooft-Veltman scheme, and more compatible with the helicity formalism, we define the *four-dimensional helicity* scheme, which has already been used in a number of one-loop calculations [5, 11, 39, 40]. The essential difference between the DR scheme and the FDH scheme is that in the former case the rules for dot products follow from taking $D < 4$ while in the latter one they follow from taking $D > 4$.

The precise rules for the four-dimensional helicity scheme are:

- As in ordinary dimensional regularization, all momentum integrals are integrated over D-component momenta. Any Kronecker δ_{μ}^{ν}'s resulting from the integration are D-dimensional. (This is necessary for maintaining gauge invariance.)

- All "observed" external states are left in four dimensions; their momenta are also four-dimensional. (In QCD the "observed" states refer to the external states appearing in the hard part of the process described by Feynman diagrams, ignoring any subsequent hadronization.) Because $D > 4$, we may view this rule as choosing momenta and polarizations to lie solely in a four-dimensional subspace. In this way it is natural to use helicity states for "observed" particles.

- All "unobserved" internal states are treated as D_s dimensional, where $D_s \geq D$ in all intermediate steps. The "unobserved" states include virtual states in loops, virtual intermediate states in trees (which may be attached to loops), as well as any external states which are in collinear or soft parts of phase space. Any explicit factors of dimension arising from the Lorentz and γ-matrix algebra should be labeled as D_s, and should be kept distinct from the dimension D describing the number of components of the loop momenta.

- Since $D > 4$, for any four-dimensional vector (such as an "observed" polarization vector or momentum), $\varepsilon_{(4)}^{\mu}$, the dot product with a D-dimensional vector yields a four-dimensional dot

9

product, $\varepsilon^\mu_{(4)} p^{(D)}_\mu = \varepsilon^\mu_{(4)} p^{(4)}_\mu$. In general, dot products of four-dimensional vectors with (-2ϵ)-dimensional ones always vanish.

Though the rules for various dot products are constructed with $D > 4$ in mind, at the end the expressions are analytic functions of D and D_s which can be continued to any desired region. By setting $D_s = D$ these rules are *precisely* the ones for the 't Hooft-Veltman scheme. The FDH scheme is specified by taking the parameter $D_s \to 4$, after all Lorentz and γ-matrix algebra has been performed.

A feature of the FDH scheme that makes it useful in QCD amplitude computations is its simple relation to the widely used 't Hooft-Veltman scheme. By keeping track of the D_s parameter when performing calculations one can easily switch between the 't Hooft-Veltman and the FDH scheme. In section 6, we will quote results in both the FDH and the 't Hooft-Veltman scheme, leaving D_s as a free parameter. In fact, one can define a continuous class of schemes by setting $D_s = 4 - 2\epsilon\, \delta_R$, as in eq. (8.5) below, though we see no particular utility to schemes other than FDH ($\delta_R = 0$) and HV ($\delta_R = 1$).

For this approach to be sensible, the coefficients of each power of D_s must be separately gauge invariant. In any theory with either gauge or Yukawa interactions, the terms with D_s in a given Feynman diagram can be mapped to another diagram where (fictitious) scalar lines replace some of the gluon lines in the diagram. After summing over diagrams, the terms with D_s to a certain power are proportional to a sum of diagrams containing a certain number of fictitious scalar loops; the sum is gauge invariant because it corresponds to a physical amplitude.

At one loop, the supersymmetry preservation properties of the FDH scheme have been verified in a number of papers [11, 35]. One of the aims of this paper is to provide explicit examples demonstrating that the FDH variant of dimensional regularization preserves the SWI (2.3) through at least two loops.

4   Cutting method

As mentioned in the introduction, we did not use Feynman diagrams directly to compute the explicit two-loop helicity amplitudes. Instead we used a cutting method [35, 41, 42], which has been applied previously to a number of one-loop calculations, including the corrections to $e^+e^- \to 4$ partons [40], and more theoretical studies, such as the construction of infinite sequences of maximally helicity violating amplitudes [35, 42] and the investigation of the divergence structure of supergravity [43]. More recently, it has also been used to produce two-loop $2 \to 2$ scattering amplitudes in super-Yang-Mills theory, QCD and QED [14, 15, 20, 21, 19]. In sect. 6 we will present the four-gluon amplitude for the $++++$ helicity configuration, in both QCD and supersymmetric theories, obtained via the cutting method. We use this amplitude to investigate the supersymmetry identities and associated regularization issues. We have also computed, by the same techniques, the $-+++$ amplitude components which do not involve scalars; they too satisfy the supersymmetry identities. The cutting method can help clarify the unitarity and gauge invariance of the regularization procedure, because the basic building blocks for loop amplitudes are gauge invariant tree-level S-matrix elements.

The cutting method amounts to an extension of traditional unitarity methods [44]. Traditional applications of unitarity in four dimensions, via dispersion relations, often suffer from subtraction ambiguities. These ambiguities are related to the appearance of rational functions with vanishing imaginary parts, $R(S_i)$, where $S_i = \{s, t, u, \ldots\}$ are the kinematic variables for the amplitude. However, dimensionally-regulated amplitudes for massless particles, as we consider here, necessarily acquire a factor of $(-S_i)^{-\epsilon}$ for each loop, from the loop integration measure $\int d^{4-2\epsilon} L$ and dimensional analysis. For small ϵ, we expand $(-S_i)^{-\epsilon} R(S_i) = R(S_i) - \epsilon \ln(-S_i) R(S_i) + \mathcal{O}(\epsilon^2)$, so every term has an imaginary part (for some $S_i > 0$), though not necessarily in those terms which survive as $\epsilon \to 0$. Thus, the unitarity cuts evaluated to $\mathcal{O}(\epsilon)$ provide sufficient information for the complete reconstruction of an amplitude through $\mathcal{O}(\epsilon^0)$, subject only to the usual prescription dependence associated with renormalization. The subtraction ambiguities that arise in traditional dispersion relations are related to the non-convergence of dispersion integrals. A dimensional regulator makes such integrals well-defined and correspondingly eliminates the subtraction ambiguities. In a sense, we use dimensional regularization as a calculational tool, beyond its usual role as an infrared and ultraviolet regulator.

It is useful to view the unitarity-based technique as an alternate way of evaluating sets of ordinary Feynman diagrams. It does this by collecting together gauge-invariant sets of terms which correspond to the residues of poles in the integrands. The poles are those of the propagators of the cut lines. This corresponds to a region of loop-momentum integration where the cut loop momenta go on shell and the corresponding internal lines become the intermediate states in a unitarity relation. From this point of view, we may consider even more restricted regions of loop momentum integration, where additional internal lines go on shell (and, if they are gluons, become transverse as well). This amounts to imposing cut conditions on additional internal lines.

Besides the more traditional two- and three-particle cuts one can define "double" two-particle generalized cuts [15] for a two-loop four-point amplitude. An example of this quantity is illustrated in fig. 3(a), and written in terms of on-shell tree amplitudes as,

$$\mathcal{A}_4^{\text{2-loop}}\Big|_{2\times 2\text{-cut}} = \sum_{\substack{\text{physical} \\ \text{states}}} \mathcal{A}_4^{\text{tree}}(1, 2, -\ell_2, -\ell_1) \times \mathcal{A}_4^{\text{tree}}(\ell_1, \ell_2, -\ell_3, -\ell_4) \times \mathcal{A}_4^{\text{tree}}(\ell_4, \ell_3, 3, 4), \qquad (4.1)$$

where the on-shell conditions $\ell_i^2 = 0$ are imposed on the ℓ_i, $i = 1, 2, 3, 4$ appearing on the right-hand side. This equation should *not* be interpreted as trying to take "the imaginary part of an imaginary part". Rather it should be understood in the sense of the previous paragraph as supplying information about the integrand of the two-loop amplitude. It supplies only part of the information contained in the usual two-particle cut, which effectively imposes only two kinematic constraints on the intermediate lines. However, it is simpler to evaluate because it is composed only of tree amplitudes. There are, of course, other ways to cut the two-loop amplitude to obtain trees. For example, in fig. 3(b) a different arrangement of the cut trees is shown,

$$\mathcal{A}_4^{\text{2-loop}}\Big|_{\text{hv-cut}} = \sum_{\substack{\text{physical} \\ \text{states}}} \mathcal{A}_4^{\text{tree}}(1, \ell_1, \ell_2, -\ell_4) \times \mathcal{A}_4^{\text{tree}}(2, -\ell_3, -\ell_2, -\ell_1) \times \mathcal{A}_4^{\text{tree}}(\ell_4, \ell_3, 3, 4). \qquad (4.2)$$

The combined set of double two-particle cuts provides all information present in the ordinary two-particle cuts (where a single pair of lines is cut, and a loop amplitude is still present), thus obviating
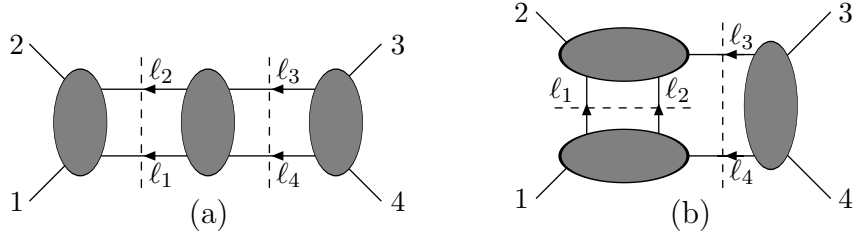
the need to evaluate such cuts.

Figure 3: Two examples of s-channel double two-particle cuts of a two-loop amplitude, which separate it into a product of three tree amplitudes. The dashed lines represent the generalized cuts.

The full amplitude, including all color factors, may be obtained by combining a suitable set of generalized cuts into a single expression whose cuts match the explicitly calculated cuts. At two loops, it is sufficient to evaluate all the double two-particle cuts with the topologies shown in fig. 3, plus the "standard" three-particle cut, shown in fig. 4 and given by

$$\mathcal{A}_4^{\text{2-loop}}\Big|_{\text{3-cut}} = \sum_{\substack{\text{physical} \\ \text{states}}} \mathcal{A}_5^{\text{tree}}(1, 2, -\ell_3, -\ell_2, -\ell_1) \times \mathcal{A}_5^{\text{tree}}(\ell_1, \ell_2, \ell_3, 3, 4) \,. \tag{4.3}$$

For the identical-helicity amplitudes discussed in this paper, the integrands are sufficiently simple that we can combine all double two-particle cuts and three-particle cuts into compact integrands containing no cut restrictions. We present these compact integrands in sect. 6.
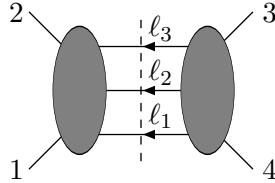

Figure 4: The standard three-particle cut of a two-loop amplitude.

To obtain and verify the compact representations of the amplitudes presented in this paper, it proved useful to compare numerically, at a number of random kinematic points, two different representations of the cut integrands ("raw" and simplified), before performing any loop integrations. This comparison is only simple to implement when the number of dimensions D is an integer. Integer values for D may seem at odds with dimensional regularization, which requires expressions to be evaluated in non-integer numbers of dimensions in order to analytically continue to $D = 4$. However, a cut integrand contains no explicit dependence on the dimension D, only that implicit in the dot products of loop momentum vectors. It is therefore sufficient to verify the cut integrands numerically for integer values of D. In so doing, we keep D_s an analytic parameter, independent of D; *i.e.*, we verify the cut integrands for all values of D_s. One should take care that the number of dimensions is no smaller than the number of independent vectors in the problem. At two loops, there are two independent loop momenta with non-vanishing components in the extra dimensions. Hence the

extra-dimensional subspace must be at least two-dimensional, for a minimum total dimension of $D = 6$. If two cut integrands agree numerically in six or more dimensions (with D_s left arbitrary), then the lack of any explicit D dependence ensures that they are identical for any value of D.

5 Color decomposition of QCD amplitudes

Gauge theory scattering amplitudes have a rich color structure. A number of different color decompositions have been used to organize this structure, particularly at the tree and one-loop level [45, 4, 46, 6, 47]. In general, an amplitude is color decomposed by writing it as a sum of terms. Each term is the product of a "color structure" and a "primitive" (or "color-stripped") amplitude. A color structure is a tensor in color space, but is independent of the momenta and polarizations of the external states. A primitive amplitude, on the other hand, contains no color indices or group theory information; it is a function only of the kinematic variables.

For gluon scattering amplitudes in $SU(N_c)$ gauge theory, "trace-based" decompositions have been used frequently [45, 4, 46, 6]. Here the color structures have the form $\mathrm{Tr}(T^{a_{i_1}} \cdots T^{a_{i_n}})$, $\mathrm{Tr}(T^{a_{i_1}} \ldots T^{a_{i_m}}) \, \mathrm{Tr}(T^{a_{i_{m+1}}} \ldots T^{a_{i_n}})$, *etc.*, where T^a is a generator in the fundamental representation. However, a color decomposition based on the Lie algebra structure constants f^{abc} [47] is more suitable for our purposes. Note that the set of color structures may be complete, that is, it may form a linearly independent basis; or it may be overcomplete, with its elements obeying linear relations. (Usually the completeness is defined with respect to an arbitrarily large value of N_c; for small N_c it may degenerate.) If the set is complete, then the primitive amplitudes are uniquely defined; if it is overcomplete, then there is some freedom in defining them, although there may still be a natural, symmetric way to do it.

The utility of primitive amplitudes in the context of supersymmetry is that they can serve as building blocks for amplitudes in disparate theories, where the matter transforms in different representations of the gauge group. If one of the theories is supersymmetric, one can express supersymmetry relations in terms of primitive amplitudes. Then the supersymmetric properties of the primitive amplitudes can be applied to non-supersymmetric theories such as QCD.

In this section, we first review tree and one-loop color decompositions, and remind the reader how they allow supersymmetry Ward identities to be applied to non-supersymmetric theories. Next we proceed to two loops. We organize the color and kinematics of the two-loop $gg \to gg$ amplitudes in a representation convenient for discussing the supersymmetry identity (2.3). For the case where all particles in the loops are in the adjoint representation, the two-loop color decomposition was given previously [43, 15]. Here we review this result and extend it to the case of matter in the fundamental representation. The sets of color structures used in both decompositions are overcomplete, and therefore the primitive amplitudes they define are not unique. However, the overcompleteness gives us the freedom to find very symmetric and compact forms for the primitive amplitudes, which do obey simple supersymmetry relations, at least for the special case of the $++++$ helicity configuration.

5.1 Color organization of tree and one-loop amplitudes

In order to explain the utility of primitive amplitudes in applying supersymmetry identities to QCD, first consider tree amplitudes. We employ an f^{abc}-based (not a trace-based) color decomposition [47], because it most closely matches the one we shall use at two loops. Using the Jacobi identity for the structure constants, the four-gluon tree amplitude can be decomposed as a sum of two terms,

$$\mathcal{A}_4^{\text{tree}}(1_g, 2_g, 3_g, 4_g) = g^2 \sum_{\sigma \in S_2} (F^{a_{\sigma(2)}} F^{a_{\sigma(3)}})_{a_1 a_4} A_4^{\text{tree}}(1_g, \sigma(2_g), \sigma(3_g), 4_g), \tag{5.1}$$

where the primitive amplitudes A_4^{tree} do not contain any color information. Here S_2 is the set of two permutations of the set $\{2, 3\}$, while $(F^a)_{bc} \equiv i\tilde{f}^{bac}$ is an $SU(N_c)$ generator for the adjoint representation,

$$\tilde{f}^{abc} \equiv \sqrt{2} f^{abc} = -i \,\text{Tr}([T^a, T^b]T^c), \tag{5.2}$$

where f^{abc} are the usual $SU(N_c)$ structure constants, and T^a are generators for the fundamental representation, normalized so that $\text{Tr}(T^a T^b) = \delta^{ab}$. Because the two color structures in eq. (5.1) are linearly independent, the SWI (2.8) for $\mathcal{A}_4^{\text{QCD tree}}$ applies separately to each primitive amplitude in eq. (5.1).

Next consider the two-gluino two-gluon tree amplitude in a supersymmetric theory. Because gluinos are in the adjoint representation, this amplitude satisfies a color decomposition equivalent to eq. (5.1),

$$\mathcal{A}_4^{\text{tree}}(1_\lambda, 2_g, 3_g, 4_\lambda) = g^2 \sum_{\sigma \in S_2} (F^{a_{\sigma(2)}} F^{a_{\sigma(3)}})_{a_1 a_4} A_4^{\text{tree}}(1_\lambda, \sigma(2_g), \sigma(3_g), 4_\lambda). \tag{5.3}$$

Compare this decomposition to the one for the two-quark two-gluon amplitude in QCD,

$$\mathcal{A}_4^{\text{tree}}(1_q, 2_g, 3_g, 4_{\bar{q}}) = g^2 \sum_{\sigma \in S_2} (T^{a_{\sigma(2)}} T^{a_{\sigma(3)}})_{i_1}{}^{\bar{i}_4} A_4^{\text{tree}}(1_q, \sigma(2_g), \sigma(3_g), 4_{\bar{q}}), \tag{5.4}$$

where the quarks, and T^{a_i}, are in the fundamental representation. The crucial point is that the A_4^{tree} appearing in eq. (5.3) are in fact identical to the A_4^{tree} appearing in eq. (5.4), as can easily be verified using Feynman diagrams. (In the double-line formalism for $SU(N_c)$, the color line running between the two gluinos is merely "stripped off" to obtain the quark amplitudes.) Thus, there is no real distinction between gluinos and quarks as far as the primitive amplitudes are concerned. Any SWI that holds for the primitive gluino amplitudes will hold for the quark ones.

Similar color decompositions hold at one loop. Consider the four-gluon amplitude. When the particle circulating in the loop is in the adjoint representation, e.g. a gluon or gluino, the decomposition is [47]

$$\mathcal{A}_4^{\text{adjoint loop}}(1, 2, 3, 4) = g^4 \left[\sum_{\sigma \in S_4/Z_4/\mathcal{R}} \text{Tr}(F^{a_{\sigma(1)}} F^{a_{\sigma(2)}} F^{a_{\sigma(3)}} F^{a_{\sigma(4)}}) A_4^{\text{1-loop}}(\sigma(1), \sigma(2), \sigma(3), \sigma(4)) \right]. \tag{5.5}$$

Here we have suppressed the gluon g labels on the external legs; σ runs over the set of permutations of $\{1, 2, 3, 4\}$, after removing those equivalent under a cyclic Z_4 permutation or the reflection $\mathcal{R}$:

14

$\{1, 2, 3, 4\} \rightarrow \{4, 3, 2, 1\}$. In comparison, the contribution of a fundamental representation particle in the loop, *e.g.* a quark, is decomposed as

$$\mathcal{A}_4^{\text{fund. loop}}(1, 2, 3, 4) = g^4 \left[\sum_{\sigma \in S_4/Z_4} \text{Tr}(T^{a_{\sigma(1)}} \ldots T^{a_{\sigma(4)}}) A_4^{\text{1-loop}}(\sigma(1), \sigma(2), \sigma(3), \sigma(4)) \right]. \quad (5.6)$$

Note that in both eqs. (5.5) and (5.6), the color factors may be read off of the appropriate one-loop "parent" diagram shown in fig. 1. One simply assigns a group theory factor of $\tilde{f}^{abc}$ or $(T^a)^i_{\bar{j}}$ for each vertex, and a factor of δ^{ab} or $\delta^{\bar{j}}_i$ for each internal line, then performs the index contractions. We shall use this diagrammatic representation of the color factors at two loops in sections 5.2 and 5.3.

Once again, using Feynman diagrams, it is straightforward to demonstrate that the primitive amplitude $A_4^{\text{1-loop}}$ appearing in the fundamental representation case (5.6) is exactly the same object appearing in the adjoint representation case (5.5), provided that the type of particle in the loop (fermion or scalar) is the same in both cases.

Because of this identification, QCD quark loop primitive amplitudes obey SWI. For example, let us apply eq. (2.3) to pure $N = 1$ supersymmetric Yang-Mills theory (SYM). Linear independence of the color factors appearing in eq. (5.5) implies that the primitive amplitudes satisfy

$$A_4^{\text{SYM 1-loop}}(1^\pm, 2^+, 3^+, 4^+) = A_4^{\text{gluon loop}}(1^\pm, 2^+, 3^+, 4^+) + A_4^{\text{fermion loop}}(1^\pm, 2^+, 3^+, 4^+) = 0, \quad (5.7)$$

where $A_4^{\text{gluon loop}}$ represents the gluon loop contribution to $A_4^{\text{1-loop}}$ in eq. (5.5), shown in fig. 1a, and $A_4^{\text{fermion loop}}$ represents the gluino loop contribution to $A_4^{\text{1-loop}}$, shown in fig. 1b. Because $A_4^{\text{fermion loop}}$ is the same for an adjoint or a fundamental representation fermion (although it gets inserted into a different color decomposition formula, (5.5) or (5.6), in the two cases), the identity

$$A_4^{\text{gluon loop}}(1^\pm, 2^+, 3^+, 4^+) = -A_4^{\text{fermion loop}}(1^\pm, 2^+, 3^+, 4^+) \quad (5.8)$$

holds even in QCD, where the fermion would be a quark. Continuing along these lines, consider the contribution of a chiral multiplet in super-QCD, consisting of a fermion and a scalar, to eq. (2.3). One obtains

$$A_4^{\text{scalar loop}}(1^\pm, 2^+, 3^+, 4^+) = -A_4^{\text{fermion loop}}(1^\pm, 2^+, 3^+, 4^+), \quad (5.9)$$

even for a non-supersymmetric gauge theory. As discussed in section 2.3, one must take the number of scalar states to match the number of fermion states on the two sides of eq. (5.9).

It is not difficult to verify that the SWI (5.8) and (5.9) are indeed satisfied. For the identical-helicity case $(++++)$, the one-loop amplitudes have a compact representation [48], similar to the one we shall use at two loops,

$$A_4^{\text{gluon loop}}(1^+, 2^+, 3^+, 4^+) = (D_s - 2) \frac{\rho}{i} \mathcal{I}_4^{\text{1-loop}}[\lambda_p^4],$$
$$A_4^{\text{fermion loop}}(1^+, 2^+, 3^+, 4^+) = -2 \frac{\rho}{i} \mathcal{I}_4^{\text{1-loop}}[\lambda_p^4], \quad (5.10)$$
$$A_4^{\text{scalar loop}}(1^+, 2^+, 3^+, 4^+) = 2 \frac{\rho}{i} \mathcal{I}_4^{\text{1-loop}}[\lambda_p^4],$$

corresponding to the three representative diagrams in fig. 1. Here

$$\rho \equiv i \frac{[1\,2]\,[3\,4]}{\langle 1\,2 \rangle\,\langle 3\,4 \rangle} \quad (5.11)$$

15

is a ubiquitous spinor product prefactor, which is a pure phase, and is totally symmetric under permutations of the external legs $\{1, 2, 3, 4\}$. The one-loop integral appearing in the amplitudes is

$$
\begin{aligned}
\mathcal{I}_4^{\text{1-loop}}[\lambda_p^4] &= \int \frac{d^D p}{(2\pi)^D} \frac{\lambda_p^4}{p^2 (p - k_1)^2 (p - k_1 - k_2)^2 (p + k_4)^2} \\
&= -\frac{i}{6} \frac{1}{(4\pi)^2} + \mathcal{O}(\epsilon),
\end{aligned}
\tag{5.12}
$$

where we have split the loop momentum $p = p_{[4]} + \vec{\lambda}_p$ into its four-dimensional components $p_{[4]}$ and its (-2ϵ)-dimensional components $\vec{\lambda}_p$, with $\lambda_p^4 \equiv (\vec{\lambda}_p \cdot \vec{\lambda}_p)^2$. (The value of $\mathcal{I}_4^{\text{1-loop}}[\lambda_p^4]$ is known through $\mathcal{O}(\epsilon^2)$ [15].) Full amplitudes, including all color factors, are obtained by substituting the primitive amplitudes in eq. (5.10) into eqs. (5.5) and (5.6).

From eq. (5.10) we see that the SWI (5.8) and (5.9) hold to all orders in ϵ in the FDH scheme, where $D_s = 4$. Note that in the HV scheme, where $D_s = 4 - 2\epsilon$, the SWI do hold at one loop *in the limit $\epsilon \to 0$* for the $++++$ (and $-+++$) helicity configurations [5]; however, the identities for the $--++$ and $-+-+$ amplitudes are known to be explicitly violated, even in this limit [11].

5.2   Purely adjoint representation two-loop color decomposition

The two-loop color decomposition we use is similar to the tree and one-loop decompositions described above. For the case where all particles are in the adjoint representation, the complete amplitude is given by

$$
\mathcal{A}_X^{\text{adjoint}} = g^6 \sum_{\{D_i\}} \left[C_{1234}^{D_i} A_{X1234}^{D_i} + C_{3421}^{D_i} A_{X3421}^{D_i} + \mathcal{C}(234) \right].
\tag{5.13}
$$

Here C^{D_i} are color factors, while A^{D_i} are primitive amplitudes. The notation "$+ \mathcal{C}(234)$" instructs one to add the two non-trivial cyclic permutations of $(2,3,4)$. To simplify the formulae, we adopt a diagrammatic representation of the color factors, in terms of a set of "parent" diagrams, depicted in figs. 5–8. The label $X = G, S, F, M$ refers to whether the contribution is respectively from gluons, adjoint scalars, adjoint fermions, or mixed fermion-scalar loop contributions, corresponding to figs. 5, 6, 7 and 8, respectively. Which of these contributions appear in the full amplitude depends, of course, on the matter content of the theory under consideration, through equations like (2.12) and (2.13).

Each color factor C^{D_i} in eq. (5.13) is specified by a parent diagram, where the corresponding label D_i is shown in parentheses in the figure. For example, the fermion loop contribution color factor $C_{1234}^{P_1}$ is found from fig. 6(P_1). The color factor is calculated from the parent diagram by associating each vertex and internal line with a color tensor, and then performing the internal index contractions. For the case where all particles are in the adjoint representation, the internal lines are "dressed" with factors of δ^{ab}. The vertex dressing rules are as follows:

- A gauge 3-point vertex is dressed with $i\tilde{f}^{abc} = \text{Tr}([T^a, T^b] T^c)$.

- A superpotential 3-point vertex is dressed with $d^{abc} \equiv \text{Tr}(\{T^a, T^b\} T^c)$.

- The 4-point vertex in the double-scalar loop diagram P_5 in fig. 7 is dressed with

  $\star \frac{1}{2} i^2 (\tilde{f}^{abe} \tilde{f}^{ecd} + \tilde{f}^{bce} \tilde{f}^{eda})$ in the case of a gauge coupling (D term), and

$\star\ d^{bce}d^{eda}$ in the case of a superpotential coupling (F term).

The structure of the 4-point vertices follows from the Lagrangian terms (2.6) and (2.7), respectively. Color factors with the legs ordered differently from the figures, such as $C^{\mathrm{P}_1}_{3421}$, are obtained by appropriate relabeling of the external legs. In the fundamental representation case to be discussed in section 5.3, the same color factor rules will hold, after correcting for the different representations; for example, $\delta_i^{\bar{\jmath}}$ should clearly be used for a fundamental line, and $(T^a)^i_{\bar{\jmath}}$ for a three-point vertex with two fundamental lines emanating from it.

The primitive amplitudes A^{D_i} are defined as the coefficients of the color factors in eq. (5.13). Actually, in contrast to the tree and one-loop cases, this prescription does not completely specify the primitive amplitudes, because the color factors in eq. (5.13) are not linearly independent (see below). Also, the quantities A_4^{tree} and $A_4^{\mathrm{1\text{-}loop}}$ can be given gauge-invariant definitions, as sums of complete sets of color-ordered Feynman diagrams. Such a definition fails here. For example, the pure glue contributions A^{P}_{G1234} and A^{P}_{G1432} both contribute at leading order in N_c to the cyclic color ordering 1234, and thus only the sum of them has a gauge-invariant definition. In any case, the primitive amplitudes A^{D_i} that we present in sect. 6 are arranged to fulfill eq. (5.13). In addition, each such A^{D_i} does include the corresponding parent diagram from figs. 5–8 in its definition; it also includes pieces of other "daughter" Feynman diagrams (not shown in the figures), which are typically shared with other primitive amplitudes.
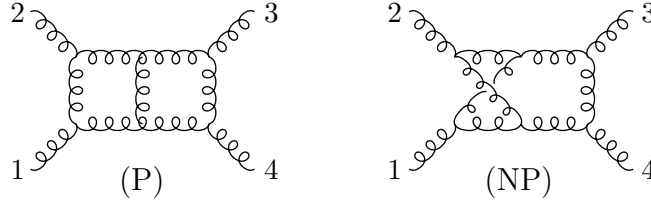

Figure 5: Parent graphs for the pure gluon G contributions.

For the purely adjoint color representation, in the gauge coupling case for which all vertices are built out of factors of $\tilde{f}^{abc}$, an equivalent but much simpler color decomposition has been given [43, 15]. This decomposition is in terms of just the color factors P and NP shown in fig. 5. Subdividing the parent diagrams D_i into planar ones P_i and non-planar ones NP_i, we have

$$\mathcal{A}_X^{\mathrm{adjoint}} = g^6 \bigg\{ \sum_{\{\mathrm{P}_i\}} \Big[C^{\mathrm{P}}_{1234} A^{\mathrm{P}_i}_{X1234} + C^{\mathrm{P}}_{3421} A^{\mathrm{P}_i}_{X3421} \Big] + \sum_{\{\mathrm{NP}_i\}} \Big[C^{\mathrm{NP}}_{1234} A^{\mathrm{NP}_i}_{X1234} + C^{\mathrm{NP}}_{3421} A^{\mathrm{NP}_i}_{X3421} \Big] + \mathcal{C}(234) \bigg\}.$$
(5.14)

In the pure gluon case, as indicated in fig. 5, we lump all of the P_i primitive amplitudes together, and similarly for the NP_i ones, so that the actual decomposition is

$$\mathcal{A}_G^{\mathrm{adjoint}} = g^6 \bigg\{ C^{\mathrm{P}}_{1234} A^{\mathrm{P}}_{G1234} + C^{\mathrm{P}}_{3421} A^{\mathrm{P}}_{G3421} + C^{\mathrm{NP}}_{1234} A^{\mathrm{NP}}_{G1234} + C^{\mathrm{NP}}_{3421} A^{\mathrm{NP}}_{G3421} + \mathcal{C}(234) \bigg\}.$$
(5.15)

The equivalence of eqs. (5.13) and (5.14) is not completely manifest. While it is clear that

$$C^{\mathrm{P}_i}_{1234} = C^{\mathrm{P}}_{1234}, \qquad C^{\mathrm{NP}_i}_{1234} = C^{\mathrm{NP}}_{1234}, \qquad i = 1, 2, 3,$$
(5.16)

17

it is also true that

$$C^{\mathrm{P}_4}_{1234} \neq C^{\mathrm{P}}_{1234} \neq C^{\mathrm{P}_5}_{1234}.$$

Nevertheless, the symmetry properties of the primitive amplitudes presented in sect. 6 are such that, after summing over the permutations in eqs. (5.13) and (5.14), the two forms are equivalent. The P_4 primitive amplitudes, after loop integration, all turn out to be proportional to the same function, which is antisymmetric under exchange of legs 1 and 2 (or 3 and 4). In the permutation sum (5.14), this property induces an antisymmetric projection on the double planar box (P) color factor, which removes certain unwanted (subleading-color) terms, and renders it equivalent to the double triangle (P_4) color factor [15]. Similarly, the double-scalar P_5 primitive amplitude is symmetric under exchange of legs 1 and 2 (or 3 and 4), and the symmetric projection on its $C^{\mathrm{P}_5}_{1234}$ color factor in eq. (5.13) renders it equivalent to C^{P}_{1234}. We emphasize that the simplified color decomposition (5.14) applies only to the pure gauge coupling, adjoint representation case, and not when either Yukawa couplings or fundamental representations are present.

The symmetries of the color factors C^{P} and C^{NP} can be read off the diagrams. The ones required in the sum (5.14) are

$$C^{\mathrm{P}}_{4321} = C^{\mathrm{P}}_{1234}\,, \qquad\qquad C^{\mathrm{NP}}_{1243} = C^{\mathrm{NP}}_{1234}\,. \qquad\qquad (5.17)$$

The corresponding planar and non-planar primitive amplitudes share the same symmetries with their associated color factors. Due to these symmetries, $\mathcal{A}^{\mathrm{adjoint}}_X(1^+,2^+,3^+,4^+)$ has the required total (S_4) permutation symmetry, even though only six permutations appear explicitly in eq. (5.14). Although diagrams with differing color factors contribute to each primitive amplitude, roughly speaking, gauge invariance dictates that in the final gauge invariant expression, all diagrams follow the lead of the parent diagrams. The final permutation sum then ensures that diagrammatic contributions with seemingly incorrect color factors receive the correct ones after assembly.

The color representation in eq. (5.14) is not unique, although it is a particularly symmetric one. Indeed, the twelve color factors appearing in eq. (5.14) or (5.15) satisfy a set of seven linear relations,

$$
\begin{aligned}
C^{\mathrm{P}}_{1234} - C^{\mathrm{P}}_{2341} = C^{\mathrm{NP}}_{1234} - C^{\mathrm{NP}}_{1423}\,, \quad C^{\mathrm{P}}_{1342} - C^{\mathrm{P}}_{3421} = C^{\mathrm{NP}}_{1342} - C^{\mathrm{NP}}_{1234}\,, \quad C^{\mathrm{P}}_{1423} - C^{\mathrm{P}}_{4231} = C^{\mathrm{NP}}_{1423} - C^{\mathrm{NP}}_{1342}\,, \\
C^{\mathrm{NP}}_{1234} = C^{\mathrm{NP}}_{3421}\,, \qquad\qquad C^{\mathrm{NP}}_{1342} = C^{\mathrm{NP}}_{4231}\,, \qquad\qquad C^{\mathrm{NP}}_{1423} = C^{\mathrm{NP}}_{2341}\,, \\
C^{\mathrm{NP}}_{1234} + C^{\mathrm{NP}}_{1342} + C^{\mathrm{NP}}_{1423} = 0\,,
\end{aligned}
$$
$$(5.18)$$

hence only five color factors are linearly independent. The amplitude (5.15) may be rewritten, for example, into the non-symmetric form,

$$
\begin{aligned}
\mathcal{A}^{\mathrm{adjoint}}_G = g^6 \Big[&C^{\mathrm{P}}_{2341}(A^{\mathrm{P}}_{G1234} + A^{\mathrm{P}}_{G2341}) + C^{\mathrm{P}}_{1342}(A^{\mathrm{P}}_{G1342} + A^{\mathrm{P}}_{G3421}) + C^{\mathrm{P}}_{1423}(A^{\mathrm{P}}_{G1423} + A^{\mathrm{P}}_{G4231}) \\
&+ C^{\mathrm{NP}}_{1423}(A^{\mathrm{NP}}_{G1423} + A^{\mathrm{NP}}_{G2341} - A^{\mathrm{NP}}_{G1234} - A^{\mathrm{P}}_{G3421} - 2A^{\mathrm{P}}_{G1234} - A^{\mathrm{P}}_{G4231}) \\
&+ C^{\mathrm{NP}}_{1342}(A^{\mathrm{NP}}_{G1342} + A^{\mathrm{NP}}_{G4231} - A^{\mathrm{NP}}_{G1234} - A^{\mathrm{P}}_{G3421} - 2A^{\mathrm{P}}_{G3421} - A^{\mathrm{P}}_{G1234} + A^{\mathrm{P}}_{G4231}) \Big].
\end{aligned}
$$
$$(5.19)$$

where each color factor is linearly independent from the others for $SU(N_c)$ for a generic value of N_c. An advantage of a linearly independent form like eq. (5.19) is that the coefficient of each color factor must satisfy supersymmetry identities by itself. The particular form (5.19) is convenient for analyzing the s-channel three-particle cuts shown in fig. 4.
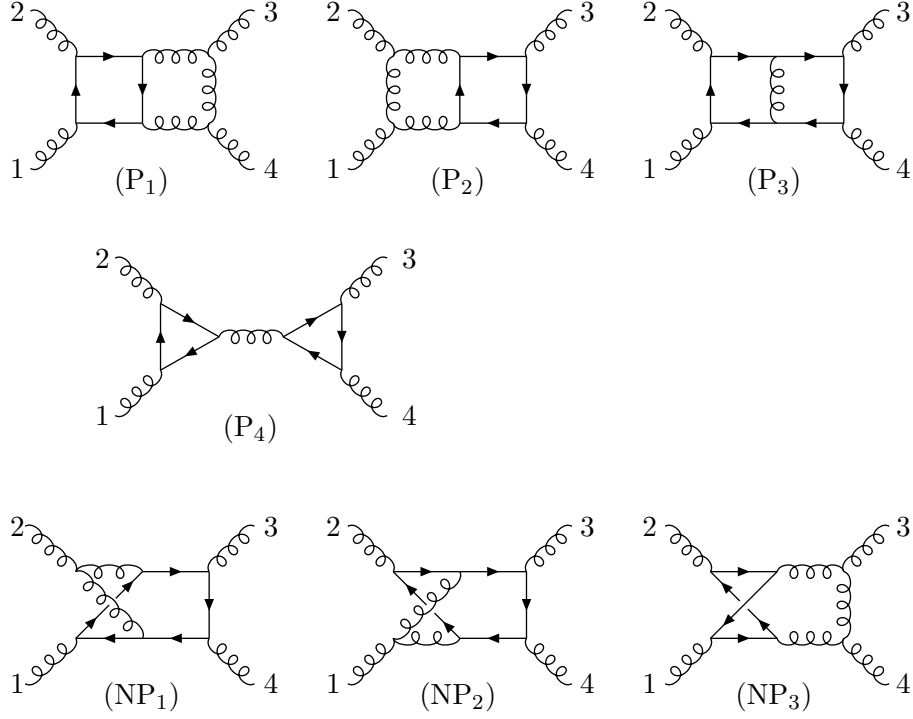
18

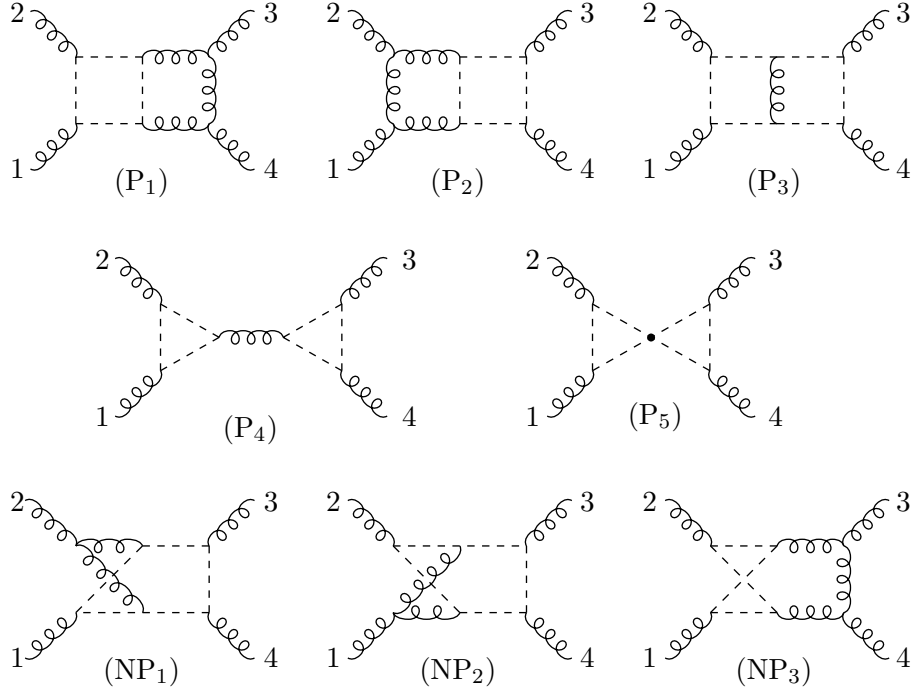Figure 6: Parent diagrams for the fermion loop F contributions.

Figure 7: Parent diagrams for the scalar loop S contributions.

We mention that although the original construction [43] of the color organization (5.15) made use of special properties of $N = 4$ supersymmetric amplitudes, the decomposition actually holds for
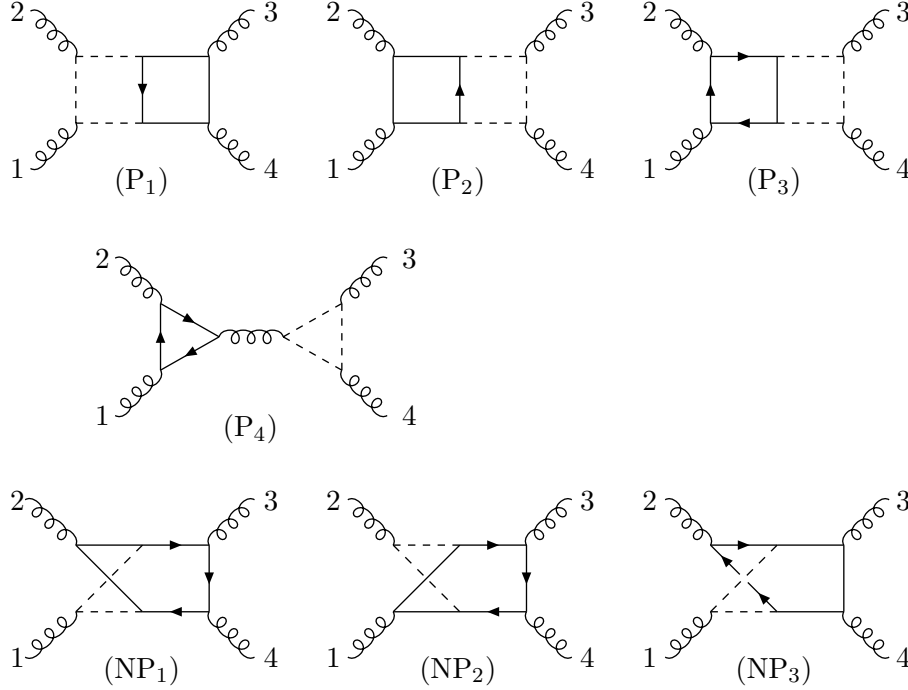
Figure 8: Parent graphs for the mixed M fermion scalar loop contributions. Diagrams P_1, P_2, P_3, NP_1, NP_2 and NP_3 contain Yukawa interactions and can contribute to either the pure gauge coupling case, or the superpotential case proportional to $|\xi|^2$; whereas diagram P_4 contributes only to the pure gauge coupling case. In the pure gauge coupling case, the solid lines with arrows represent matter fermions and the solid lines with no arrows gluinos. In each case there are additional contributions obtained from swapping the scalar lines with the matter fermion lines, but this swap does not alter the color factor.

any purely adjoint two-loop amplitude, as long as all vertices are built out of $\tilde{f}^{abc}$ factors. In such cases, one can make use of the Jacobi identity to rearrange the color factor of any Feynman diagram into a combination of those appearing in eq. (5.15) [47].

5.3 Fundamental representation two-loop color decomposition

The color decomposition for four-gluon two-loop amplitudes containing fundamental representation particles in the loops is similar to the purely adjoint case (5.13),

$$\mathcal{A}_X^{\text{fund}} = g^6 \sum_{\{\text{D}_i\}} \left[\left(F_{1234}^{\text{D}_i} A_{X1234}^{\text{D}_i} + F_{3421}^{\text{D}_i} A_{X3421}^{\text{D}_i} \right) + \mathcal{C}(234) \right], \tag{5.20}$$

where each term in the sum corresponds to a parent diagram in figs. 6–10. In this case, it is useful to include separate $\tilde{S}$ and $\tilde{F}$ contributions with a closed gluino loop, and either a closed matter fermion or a closed scalar loop, as depicted in figs. 9 and 10. Again the label $X \in \{S, F, M, \tilde{S}, \tilde{F}\}$ specifies the figure containing the parent diagram. The values of the F^{D_i} fundamental representation color coefficients are read off from these figures by dressing the parent diagrams with standard Feynman rule color factors, as in sect. 5.2 but taking into account the different representations here. For example, for the fermion loop F amplitudes, the color factor associated with each primitive amplitude is obtained by assigning an $\tilde{f}^{abc}$ to each three-gluon vertex and a $(T^a)^i_j$ to each quark-

anti-quark-gluon vertex, and summing over the two directions of the fermion arrows.

The color factors obtained by dressing the P_1 and P_2 diagrams in figs. 9 and 10 with $\tilde{f}^{abc}$ and $(T^a)^i_{\bar{j}}$ factors are not equal to the color factors $F^{P_1}_{1234}$ or $F^{P_2}_{1234}$ obtained from figs. 6–8; they differ in the $\mathrm{Tr}(T^{a_1}T^{a_2})\,\mathrm{Tr}(T^{a_3}T^{a_4})$ term. Nevertheless, after the permutation sum in eq. (5.20), this discrepancy cancels, in the same way that the discrepancy between $C^{P_4}_{1234}$ and C^P_{1234} cancelled in the purely adjoint representation case. This feature allows us to maintain a uniform set of color factors for all contributions with fundamental representation matter; *i.e.*, in eq. (5.20) there is no need to include an X label on the color factors.
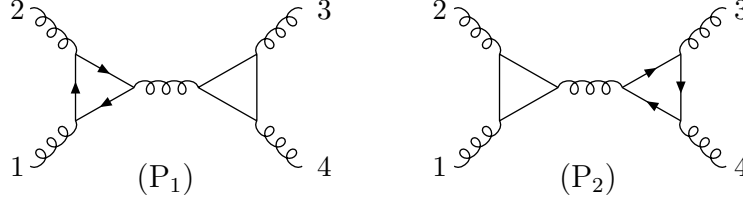

Figure 9: The $\tilde{F}$ contributions with a closed fundamental representation matter fermion loop and a closed gluino loop. The lines with the arrows represent matter fermions.
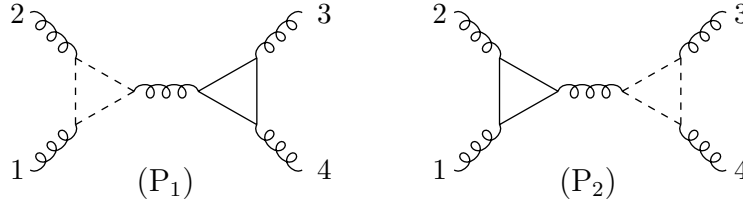

Figure 10: The $\tilde{S}$ contributions with a closed fundamental representation matter scalar loop and a closed gluino loop.

For the fundamental representation contributions to the four-gluon amplitudes, the explicit values of the color factors are

$$
\begin{aligned}
F^{P_1}_{1234} &= F^{P_2}_{1234} = N_c\left[\,\mathrm{Tr}(T^{a_1}T^{a_2}T^{a_3}T^{a_4}) + \mathrm{Tr}(T^{a_4}T^{a_3}T^{a_2}T^{a_1})\right] + 2\,\mathrm{Tr}(T^{a_1}T^{a_2})\,\mathrm{Tr}(T^{a_3}T^{a_4})\,, \\
F^{P_3}_{1234} &= F^{P_5}_{1234} = -\frac{1}{N_c}\left[\,\mathrm{Tr}(T^{a_1}T^{a_2}T^{a_3}T^{a_4}) + \mathrm{Tr}(T^{a_4}T^{a_3}T^{a_2}T^{a_1})\right] + 2\,\mathrm{Tr}(T^{a_1}T^{a_2})\,\mathrm{Tr}(T^{a_3}T^{a_4})\,, \\
F^{P_4}_{1234} &= \mathrm{Tr}(T^{a_1}T^{a_2}T^{a_3}T^{a_4}) + \mathrm{Tr}(T^{a_4}T^{a_3}T^{a_2}T^{a_1}) - \frac{2}{N_c}\,\mathrm{Tr}(T^{a_1}T^{a_2})\,\mathrm{Tr}(T^{a_3}T^{a_4})\,, \\
F^{NP_1}_{1234} &= F^{NP_2}_{1234} = 2\,\mathrm{Tr}(T^{a_1}T^{a_2})\,\mathrm{Tr}(T^{a_3}T^{a_4})\,, \\
F^{NP_3}_{1234} &= -2\left[\,\mathrm{Tr}(T^{a_1}T^{a_3})\,\mathrm{Tr}(T^{a_2}T^{a_4}) + \mathrm{Tr}(T^{a_1}T^{a_4})\,\mathrm{Tr}(T^{a_2}T^{a_3})\right]\,.
\end{aligned}
\tag{5.21}
$$

We have dropped terms containing $\mathrm{Tr}(T^{a_i})$ from eq. (5.21), since they vanish for $SU(N_c)$ gluons. Such terms would have to be restored in order to describe two-loop amplitudes with a mixture of external gluons and photons, as in ref. [20].

As in the case of the adjoint representation color decomposition (5.14), the decomposition (5.20) is not unique; there are linear relations between the various color factors. In particular, in the case of four external gluons, after eliminating redundant color factors, using the explicit representation

of the color factors in terms of color traces (5.21), one finds a total of six independent color factors. Also note that the separation into primitive amplitudes is in many cases artificial. For example, since $F^{P_1}_{1234} = F^{P_2}_{1234}$, the distinction between $A^{P_1}_{1234}$ and $A^{P_2}_{1234}$ is moot, when all four external legs are gluons.

5.4   Assembly of complete amplitudes

We can specify the amplitudes in various theories in terms of the primitive amplitudes introduced above, and presented in sect. 6 for the $++++$ helicity configuration. For example, the four-gluon amplitude in QCD with n_f massless quark flavors is,

$$\mathcal{A}_{\text{QCD}} = \mathcal{A}^{\text{adjoint}}_G + n_f \mathcal{A}^{\text{fund}(1)}_F + n_f^2 \mathcal{A}^{\text{fund}(2)}_F. \tag{5.22}$$

The pure glue contribution $\mathcal{A}^{\text{adjoint}}_G$ is given in terms of primitive amplitudes via eq. (5.15), where the sum in that equation runs over the two diagrams in fig. 5. Similarly, the single quark loop contribution $\mathcal{A}^{\text{fund}(1)}_F$ is given via eq. (5.20), where the sum runs over all diagrams in fig. 6 except (P_4), which gives the double quark loop contribution $\mathcal{A}^{\text{fund}(2)}_F$.

Using the supersymmetric Lagrangians in sect. 2 as a guide, we may combine the primitive amplitudes given in sect. 6 into supersymmetric combinations, which must satisfy the SWI (2.3). The amplitude for $N = 1$ super-QCD with n_f matter multiplets in the fundamental representation is,

$$\begin{aligned}
\mathcal{A}_{N=1} = {} & \mathcal{A}^{\text{adjoint}}_G + \mathcal{A}^{\text{adjoint}}_F \\
& + n_f \left(\mathcal{A}^{\text{fund}(1)}_F + \mathcal{A}^{\text{fund}(1)}_S + \mathcal{A}^{\text{fund}(1)}_M + \mathcal{A}^{\text{fund}(1)}_{\tilde{F}} + \mathcal{A}^{\text{fund}(1)}_{\tilde{S}} \right) \\
& + n_f^2 \left(\mathcal{A}^{\text{fund}(2)}_F + \mathcal{A}^{\text{fund}(2)}_S + \mathcal{A}^{\text{fund}(2)}_M \right),
\end{aligned} \tag{5.23}$$

which is expressed in terms of primitive amplitudes via eqs. (5.14), (5.15), and (5.20). The sum over parent diagrams of the form A_{1234} for each contribution is

$$\begin{aligned}
\mathcal{A}^{\text{adjoint}}_G &: \text{Fig. 5} , \{D_i\} = \{\text{P}, \text{NP}\}, \\
\mathcal{A}^{\text{adjoint}}_F &: \text{Fig. 6} , \{D_i\} = \{\text{P}_1, \text{P}_2, \text{P}_3, \text{P}_4, \text{NP}_1, \text{NP}_2, \text{NP}_3\}, \\
\mathcal{A}^{\text{fund}(1)}_F &: \text{Fig. 6} , \{D_i\} = \{\text{P}_1, \text{P}_2, \text{P}_3, \text{NP}_1, \text{NP}_2, \text{NP}_3\}, \\
\mathcal{A}^{\text{fund}(1)}_S &: \text{Fig. 7} , \{D_i\} = \{\text{P}_1, \text{P}_2, \text{P}_3, \text{P}_5, \text{NP}_1, \text{NP}_2, \text{NP}_3\}, \\
\mathcal{A}^{\text{fund}(1)}_M &: \text{Fig. 8} , \{D_i\} = \{\text{P}_1, \text{P}_2, \text{P}_3, \text{NP}_1, \text{NP}_2, \text{NP}_3\}, \\
\mathcal{A}^{\text{fund}(1)}_{\tilde{F}} &: \text{Fig. 9} , \{D_i\} = \{\text{P}_1, \text{P}_2\}, \\
\mathcal{A}^{\text{fund}(1)}_{\tilde{S}} &: \text{Fig. 10} , \{D_i\} = \{\text{P}_1, \text{P}_2\}, \\
\mathcal{A}^{\text{fund}(2)}_F &: \text{Fig. 6} , \{D_i\} = \{\text{P}_4\}, \\
\mathcal{A}^{\text{fund}(2)}_S &: \text{Fig. 7} , \{D_i\} = \{\text{P}_4\}, \\
\mathcal{A}^{\text{fund}(2)}_M &: \text{Fig. 8} , \{D_i\} = \{\text{P}_4\}.
\end{aligned} \tag{5.24}$$

Note that $\mathcal{A}^{\text{fund}(2)}_S$ does not receive a contribution from P_5 because of a cancellation between fields A_i and $\tilde{A}_i$ circulating in one of the loops.

For the case of a matter multiplet in the adjoint representation and the superpotential $W = \frac{1}{3}g\xi \, \mathrm{Tr}\Phi^3$, the contributions depending on ξ are

$$\mathcal{A}_{N=1}^{\mathrm{Yukawa}} = |\xi|^2(\mathcal{A}_S^{\mathrm{Yukawa}} + \mathcal{A}_M^{\mathrm{Yukawa}}), \qquad (5.25)$$

where the contributing parent diagrams are,

$$\begin{aligned}
\mathcal{A}_S^{\mathrm{Yukawa}} &: \mathrm{Fig.}\ 7\ , \{D_i\} = \{P_5\}\,, \\
\mathcal{A}_M^{\mathrm{Yukawa}} &: \mathrm{Fig.}\ 8\ , \{D_i\} = \{P_1, P_2, P_3, NP_1, NP_2, NP_3\}\,.
\end{aligned} \qquad (5.26)$$

In eq. (5.25), the implicit color factors appearing are generated by the "dressing rules" given in sect. 5.2.

One can also consider theories with a higher degree of supersymmetry. For example, a pure $N = 2$ super-Yang-Mills theory contains an $N = 2$ vector supermultiplet composed of a vector, two gluinos and two scalar states. This content can be viewed as an $N = 1$ theory with one adjoint matter multiplet. Modifying eq. (5.23) for $n_f = 1$, the pure $N = 2$ amplitude is

$$\begin{aligned}
\mathcal{A}_{N=2} &= \mathcal{A}_G^{\mathrm{adjoint}} + \mathcal{A}_F^{\mathrm{adjoint}} + \mathcal{A}_F^{\mathrm{adjoint}(1)} + \mathcal{A}_S^{\mathrm{adjoint}(1)} + \mathcal{A}_M^{\mathrm{adjoint}(1)} \\
&\quad + \mathcal{A}_{\tilde{F}}^{\mathrm{adjoint}(1)} + \mathcal{A}_{\tilde{S}}^{\mathrm{adjoint}(1)} + \mathcal{A}_F^{\mathrm{adjoint}(2)} + \mathcal{A}_S^{\mathrm{adjoint}(2)} + \mathcal{A}_M^{\mathrm{adjoint}(2)} \\
&= \mathcal{A}_G^{\mathrm{adjoint}} + 2\,\mathcal{A}_F^{\mathrm{adjoint}(1)} + \mathcal{A}_S^{\mathrm{adjoint}(1)} + \mathcal{A}_M^{\mathrm{adjoint}(1)} + 4\,\mathcal{A}_F^{\mathrm{adjoint}(2)} + \mathcal{A}_S^{\mathrm{adjoint}(2)} + 2\,\mathcal{A}_M^{\mathrm{adjoint}(2)}\,.
\end{aligned} \qquad (5.27)$$

In the second step we have used trivial identities for the adjoint representation,

$$\begin{aligned}
\mathcal{A}_F^{\mathrm{adjoint}} &= \mathcal{A}_F^{\mathrm{adjoint}(1)} + \mathcal{A}_F^{\mathrm{adjoint}(2)}\,, \\
\mathcal{A}_{\tilde{F}}^{\mathrm{adjoint}(1)} &= 2\,\mathcal{A}_F^{\mathrm{adjoint}(2)}\,, \\
\mathcal{A}_{\tilde{S}}^{\mathrm{adjoint}(1)} &= \mathcal{A}_M^{\mathrm{adjoint}(2)}\,.
\end{aligned} \qquad (5.28)$$

The contributing parent diagrams for $\mathcal{A}_X^{\mathrm{adjoint}(i)}$ are the same as for $\mathcal{A}_X^{\mathrm{fund}(i)}$ in eq. (5.24), except that the associated color factors are the ones for the adjoint representation, $i.e.$, $C_{1234}^{D_i}$. (For the $N = 2$ case, the arrows on the fermion lines in the figures are not important, although in fig. 8 they can be used to distinguish between the two species of gluinos.)

6 Identical-helicity two-loop amplitudes

In this section we review the results previously obtained for the pure gluon and scalar loop contributions to the $++++$ helicity amplitude [15]. Then we present our results for the QCD fermion loop contributions, followed by the contributions involving Yukawa couplings, which contribute to some of the supersymmetry Ward identities. The amplitudes presented in this section have not been renormalized; in sect. 8 we discuss their renormalization. The overall normalization of the primitive amplitudes below are such that for the gauge case they can be inserted directly into eqs. (5.13) and (5.20) without any additional combinatoric factors.c

6.1 Pure glue primitive amplitudes

Using eq. (5.15), the pure gluon two-loop amplitudes are conveniently expressed in terms of planar and non-planar primitive amplitudes whose explicit values are [15]:

$$
A_{G1234}^{\mathrm{P}} = \rho \Bigg\{ s_{12} \, \mathcal{I}_4^{\mathrm{P}} \Big[(D_s - 2)(\lambda_p^2 \lambda_q^2 + \lambda_p^2 \lambda_{p+q}^2 + \lambda_q^2 \lambda_{p+q}^2) + 16\Big((\lambda_p \cdot \lambda_q)^2 - \lambda_p^2 \lambda_q^2 \Big) \Big] (s_{12}, s_{23})
$$
$$
+ 4\,(D_s - 2)\, \mathcal{I}_4^{\mathrm{bow\text{-}tie}} [(\lambda_p^2 + \lambda_q^2)\,(\lambda_p \cdot \lambda_q)](s_{12}) \tag{6.1}
$$
$$
+ \frac{(D_s - 2)^2}{s_{12}} \, \mathcal{I}_4^{\mathrm{bow\text{-}tie}} \Big[\lambda_p^2 \lambda_q^2 \,((p+q)^2 + s_{12}) \Big] (s_{12}, s_{23}) \Bigg\},
$$

$$
A_{G1234}^{\mathrm{NP}} = \rho \, s_{12} \mathcal{I}_4^{\mathrm{NP}} \Big[(D_s - 2)(\lambda_p^2 \lambda_q^2 + \lambda_p^2 \lambda_{p+q}^2 + \lambda_q^2 \lambda_{p+q}^2) + 16\Big((\lambda_p \cdot \lambda_q)^2 - \lambda_p^2 \lambda_q^2 \Big) \Big] (s_{12}, s_{23}) , \tag{6.2}
$$

where the parent diagrams corresponding to these two primitive amplitudes are displayed in fig. 5, and ρ is defined in eq. (5.11). The other primitive amplitudes appearing in eq. (5.15) are just relabelings of these two basic ones.

The two-loop momentum integrals appearing in eqs. (6.1) and (6.2) are defined as follows. The planar double box integral

$$
\mathcal{I}_4^{\mathrm{P}}[\mathcal{P}(\lambda_i, p, q, k_i)](s_{12}, s_{23})
$$
$$
\equiv \int \frac{d^D p}{(2\pi)^D} \frac{d^D q}{(2\pi)^D} \frac{\mathcal{P}(\lambda_i, p, q, k_i)}{p^2 \, q^2 \, (p+q)^2 (p - k_1)^2 \, (p - k_1 - k_2)^2 \, (q - k_4)^2 \, (q - k_3 - k_4)^2} \tag{6.3}
$$

is displayed in fig. 11(a). The numerator factor $\mathcal{P}(\lambda_i, p, q, k_i)$ is a polynomial in the momenta. The vectors $\vec{\lambda}_p$, $\vec{\lambda}_q$ represent the (-2ϵ)-dimensional components of the loop momenta p and q. We also define $\lambda_p^2 \equiv \vec{\lambda}_p \cdot \vec{\lambda}_p \geq 0$, $\lambda_q^2 \equiv \vec{\lambda}_q \cdot \vec{\lambda}_q$, and $\lambda_{p+q}^2 \equiv (\vec{\lambda}_p + \vec{\lambda}_q)^2 = \lambda_p^2 + \lambda_q^2 + 2\vec{\lambda}_p \cdot \vec{\lambda}_q$. The bow-tie integral $\mathcal{I}_4^{\mathrm{bow\text{-}tie}}$ shown in fig. 11(c) is defined by

$$
\mathcal{I}_4^{\mathrm{bow\text{-}tie}}[\mathcal{P}(\lambda_i, p, q, k_i)](s_{12})
$$
$$
\equiv \int \frac{d^D p}{(2\pi)^D} \frac{d^D q}{(2\pi)^D} \frac{\mathcal{P}(\lambda_i, p, q, k_i)}{p^2 \, q^2 \, (p - k_1)^2 \, (p - k_1 - k_2)^2 \, (q - k_4)^2 \, (q - k_3 - k_4)^2} . \tag{6.4}
$$

The non-planar double box integral, depicted in fig. 11(b), is given by

$$
\mathcal{I}_4^{\mathrm{NP}}[\mathcal{P}(\lambda_i, p, q, k_i)](s_{12}, s_{23})
$$
$$
\equiv \int \frac{d^D p}{(2\pi)^D} \frac{d^D q}{(2\pi)^D} \frac{\mathcal{P}(\lambda_i, p, q, k_i)}{p^2 \, q^2 \, (p+q)^2 (p - k_1)^2 \, (q - k_2)^2 \, (p + q + k_3)^2 \, (p + q + k_3 + k_4)^2} . \tag{6.5}
$$

The explicit values of the integrals, as a Laurent series in ϵ through $\mathcal{O}(\epsilon^0)$, and expressed in terms of polylogarithms [49], may be found in appendix A of ref. [15]. We have checked that these values agree with results obtained using general integration methods [22, 23, 24, 25, 26, 27]. The integral

$$
\mathcal{I}_4^{\mathrm{bow\text{-}tie}}[(\lambda_p^2 + \lambda_q^2)\,(\lambda_p \cdot \lambda_q)](s_{12}) , \tag{6.6}
$$

in eq. (6.1) vanishes identically, due to antisymmetry of its integrand in $\vec{\lambda}_p \to -\vec{\lambda}_p$. However, in constructing a consistent set of cut integrands it is useful to keep it around, as well as related integrals found in the next subsections.
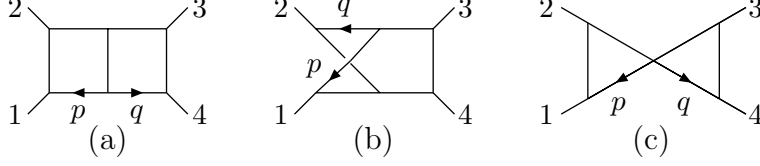
Figure 11: Integral topologies appearing in the two-loop identical-helicity amplitudes, and the loop momentum routings: (a) the planar double box integral; (b) the non-planar double box integral; (c) the bow-tie integral. The arrows here denote the direction of momentum flow.

6.2 Scalar loop primitive amplitudes

The planar scalar loop amplitudes have already been presented in ref. [15], where they were used as a guide for the construction of the pure glue amplitudes discussed above. Here we reorganize the results a bit to be compatible with eq. (5.20) for the full amplitudes for the case of fundamental representation scalars. We also present the non-planar contributions.

The scalar loop primitive amplitudes corresponding to the planar parent graphs in fig. 7 are,

$$
\begin{aligned}
A_{S1234}^{\mathrm{P}_1} = 2\rho\Big\{ & s_{12}\, \mathcal{I}_4^{\mathrm{P}}[\lambda_p^2\, \lambda_{p+q}^2](s_{12}, s_{23}) \\
& + \frac{(D_s-2)}{s_{12}}\, \mathcal{I}_4^{\text{bow-tie}}[\lambda_p^2\, \lambda_q^2\,((p+q)^2 + s_{12})](s_{12}, s_{23}) \\
& + 4\,\mathcal{I}_4^{\text{bow-tie}}[\lambda_p^2\,(\lambda_p \cdot \lambda_q)](s_{12}) \Big\}, \\
A_{S1234}^{\mathrm{P}_2} = 2\rho\Big\{ & s_{12}\, \mathcal{I}_4^{\mathrm{P}}[\lambda_q^2\, \lambda_{p+q}^2](s_{12}, s_{23}) \\
& + \frac{(D_s-2)}{s_{12}}\, \mathcal{I}_4^{\text{bow-tie}}[\lambda_p^2\, \lambda_q^2\,((p+q)^2 + s_{12})](s_{12}, s_{23}) \\
& + 4\,\mathcal{I}_4^{\text{bow-tie}}[\lambda_q^2\,(\lambda_p \cdot \lambda_q)](s_{12}) \Big\}, \\
A_{S1234}^{\mathrm{P}_3} = 2\rho\Big\{ & s_{12}\, \mathcal{I}_4^{\mathrm{P}}[\lambda_p^2\lambda_q^2](s_{12}, s_{23}) + \frac{1}{2}\mathcal{I}_4^{\text{bow-tie}}[\lambda_p^2\lambda_q^2](s_{12}) \Big\}, \\
A_{S1234}^{\mathrm{P}_4} = & \frac{4\rho}{s_{12}}\, \mathcal{I}_4^{\text{bow-tie}}\Big[\lambda_p^2\, \lambda_q^2\,((p+q)^2 + \tfrac{1}{2}s_{12})\Big](s_{12}, s_{23}), \\
A_{S1234}^{\mathrm{P}_5} = & \rho\, \mathcal{I}_4^{\text{bow-tie}}[\lambda_p^2\, \lambda_q^2](s_{12}).
\end{aligned}
\tag{6.7}
$$

Similarly, the scalar loop primitive amplitudes corresponding to the non-planar parent graphs in fig. 7 are,

$$
\begin{aligned}
A_{S1234}^{\mathrm{NP}_1} &= 2\rho\, s_{12}\, \mathcal{I}_4^{\mathrm{NP}}[\lambda_p^2\, \lambda_{p+q}^2](s_{12}, s_{23}), \\
A_{S1234}^{\mathrm{NP}_2} &= 2\rho\, s_{12}\, \mathcal{I}_4^{\mathrm{NP}}[\lambda_q^2\, \lambda_{p+q}^2](s_{12}, s_{23}), \\
A_{S1234}^{\mathrm{NP}_3} &= 2\rho\, s_{12}\, \mathcal{I}_4^{\mathrm{NP}}[\lambda_p^2\lambda_q^2](s_{12}, s_{23}).
\end{aligned}
\tag{6.8}
$$

The integrals appearing in eqs. (6.7) and (6.8) appear in the pure gluon case as well; see appendix A of ref. [15] for their explicit values through $\mathcal{O}(\epsilon^0)$. We remind the reader that the number of scalar states propagating in the above primitive amplitudes is $2 \times (N_c^2 - 1)$ in the adjoint representation case (when they are dressed with color using eq. (5.13)), and $4 \times N_c$ states for the $N_c + \bar{N}_c$ fundamental

25

representation case (when they are dressed with color using eq. (5.20)). In either case, this number matches the number of states of the fermion superpartners in the fermion loop primitive amplitudes presented in sect. 6.3.

A convenient way of organizing the numerators of the planar and non-planar double box integrals is in terms of the labels of particles circulating in the loops. Because the external momenta k_1, k_2, k_3, k_4 are defined to have vanishing extra dimensional components, as one follows a scalar line around only two different extra dimensional momenta appear, which we can label by λ_{s_1} and λ_{s_2}. For example, in fig. 7(P$_3$) the two distinct extra dimensional scalar momenta are λ_p and λ_q. Using these labels, the numerator arguments of the planar and non-planar double box integrals in eqs. (6.7) and (6.8) all have a uniform structure,

$$\lambda_{s_1}^2 \lambda_{s_2}^2 \,. \tag{6.9}$$

This observation simplifies the bookkeeping when evaluating the three-particle cuts.

6.3 Fermion loop primitive amplitudes

The structure of the fermion loop primitive amplitudes is quite similar to that of the scalar loop primitive amplitudes. The parent diagrams are described by fig. 6, and the results are,

$$
\begin{aligned}
A_{F1234}^{\mathrm{P}_1} = \rho\Big\{ & s_{12}\, \mathcal{I}_4^{\mathrm{P}}\Big[-\tfrac{1}{2}(D_s - 2)(\lambda_{p+q}\cdot\lambda_p\lambda_q^2) - 2\lambda_p^2\lambda_{p+q}^2 - 4((\lambda_p\cdot\lambda_q)^2 - \lambda_p^2\lambda_q^2)\Big](s_{12}, s_{23}) \\
& - 2\frac{D_s - 2}{s_{12}}\, \mathcal{I}_4^{\text{bow-tie}}[\lambda_p^2\lambda_q^2((p+q)^2 + s_{12})](s_{12}, s_{23}) \\
& - (D_s + 6)\, \mathcal{I}_4^{\text{bow-tie}}[\lambda_q^2\lambda_p\cdot\lambda_q](s_{12})\Big\}, \\[4pt]
A_{F1234}^{\mathrm{P}_2} = \rho\Big\{ & s_{12}\, \mathcal{I}_4^{\mathrm{P}}\Big[-\tfrac{1}{2}(D_s - 2)(\lambda_{p+q}\cdot\lambda_q\lambda_p^2) - 2\lambda_q^2\lambda_{p+q}^2 - 4((\lambda_p\cdot\lambda_q)^2 - \lambda_p^2\lambda_q^2)\Big](s_{12}, s_{23}) \\
& - 2\frac{D_s - 2}{s_{12}}\, \mathcal{I}_4^{\text{bow-tie}}[\lambda_p^2\lambda_q^2((p+q)^2 + s_{12})](s_{12}, s_{23}) \\
& - (D_s + 6)\, \mathcal{I}_4^{\text{bow-tie}}[\lambda_p^2\lambda_p\cdot\lambda_q](s_{12})\Big\}, \\[4pt]
A_{F1234}^{\mathrm{P}_3} = \rho\Big\{ & s_{12}\, \mathcal{I}_4^{\mathrm{P}}\Big[\tfrac{1}{2}(D_s - 2)(\lambda_p\cdot\lambda_q\lambda_{p+q}^2) - 2\lambda_p^2\lambda_q^2 - 4((\lambda_p\cdot\lambda_q)^2 - \lambda_p^2\lambda_q^2)\Big](s_{12}, s_{23}) \\
& + \Big(\tfrac{1}{2}(D_s - 2) - 2\Big)s_{12}\, \mathcal{I}_4^{\text{bow-tie}}[\lambda_p\cdot\lambda_q](s_{12}) + (D_s - 2)\, \mathcal{I}_4^{\text{bow-tie}}[\lambda_p^2\lambda_q^2](s_{12})\Big\}, \\[4pt]
A_{F1234}^{\mathrm{P}_4} = \rho\Big\{ & \mathcal{I}_4^{\text{bow-tie}}\Big[(\lambda_p\cdot\lambda_q)[2(\lambda_p^2 + \lambda_q^2) - \tfrac{1}{2}s_{12}]\Big](s_{12}) \\
& + \frac{4}{s_{12}}\mathcal{I}_4^{\text{bow-tie}}\Big[\lambda_p^2\lambda_q^2((p+q)^2 + \tfrac{1}{2}s_{12})\Big](s_{12}, s_{23})\Big\},
\end{aligned}
\tag{6.10}
$$

$$
\begin{aligned}
A_{F1234}^{\mathrm{NP}_1} &= \rho\, s_{12}\, \mathcal{I}_4^{\mathrm{NP}}[-\tfrac{1}{2}(D_s - 2)(\lambda_{p+q}\cdot\lambda_p\lambda_q^2) - 2\lambda_p^2\lambda_{p+q}^2 - 4((\lambda_p\cdot\lambda_q)^2 - \lambda_p^2\lambda_q^2)](s_{12}, s_{23})\,, \\
A_{F1234}^{\mathrm{NP}_2} &= \rho\, s_{12}\, \mathcal{I}_4^{\mathrm{NP}}[-\tfrac{1}{2}(D_s - 2)(\lambda_{p+q}\cdot\lambda_q\lambda_p^2) - 2\lambda_q^2\lambda_{p+q}^2 - 4((\lambda_p\cdot\lambda_q)^2 - \lambda_p^2\lambda_q^2)](s_{12}, s_{23})\,, \\
A_{F1234}^{\mathrm{NP}_3} &= \rho\, s_{12}\, \mathcal{I}_4^{\mathrm{NP}}[\tfrac{1}{2}(D_s - 2)(\lambda_p\cdot\lambda_q\lambda_{p+q}^2) - 2\lambda_p^2\lambda_q^2 - 4((\lambda_p\cdot\lambda_q)^2 - \lambda_p^2\lambda_q^2)](s_{12}, s_{23})\,.
\end{aligned}
\tag{6.11}
$$

As was the case for the scalar loop amplitudes, the normalization of the fermion loop amplitudes (when dressed with color using eqs. (5.13) and (5.20)) corresponds to $2 \times (N_c^2 - 1)$ states for the

adjoint representation case and $4 \times N_c$ states for the $N_c + \overline{N}_c$ fundamental representation case. Most of the integrals in eqs. (6.10) and (6.11) are again the same ones as for the pure glue case [15]. There are, however, a few new integrals. In ref. [19] these amplitudes, together with the other helicity configurations, are given directly in terms of polylogarithms, after subtracting off certain universal pole terms in ϵ [50].

Just as we did for the scalar loop amplitudes, we can write the numerator arguments of the loop integrals in terms of the two distinct extra-dimensional momenta flowing in the fermion propagators, which we call λ_{f_1} and λ_{f_2}, and the one in the internal gluon propagator, labeled as λ_g. In this case, the numerators appearing in the planar and non-planar double-box integrals all have the form,

$$-\tfrac{1}{2}(D_s - 2)(\lambda_{f_1} \cdot \lambda_{f_2} \lambda_g^2) - 2\lambda_{f_1}^2 \lambda_{f_2}^2 - 4((\lambda_{f_1} \cdot \lambda_{f_2})^2 - \lambda_{f_1}^2 \lambda_{f_2}^2)\,, \tag{6.12}$$

using the fact that

$$(\lambda_p \cdot \lambda_q)^2 - \lambda_p^2 \lambda_q^2 \;=\; (\lambda_{p+q} \cdot \lambda_p)^2 - \lambda_{p+q}^2 \lambda_p^2 \;=\; (\lambda_{p+q} \cdot \lambda_q)^2 - \lambda_{p+q}^2 \lambda_q^2\,. \tag{6.13}$$

6.4 Mixed scalar and fermion amplitudes

In order to fully study the supersymmetry Ward identities, we need also the "mixed" contributions where both fermions and scalars appear in the loops. The parent diagrams associated with these contributions are shown in figure 8. In these diagrams, the solid line represents fermions, while the dashed line represents scalars. These diagrams, and primitive amplitudes, describe the pure gauge coupling contributions $\mathcal{A}_M^{\text{fund}}$, for which one of the fermions is a gluino, via eq. (5.24). They simultaneously describe the superpotential (ξ-dependent) contributions, for which both of the fermions are matter fermions, via eq. (5.26).

Following the notation of the previous sections we find that the explicit forms of the planar mixed primitive amplitudes are

$$A_{M1234}^{\text{P}_1} = \rho\Big\{ s_{12}\, \mathcal{I}_4^{\text{P}}[\lambda_p \cdot \lambda_q \lambda_{p+q}^2 - \lambda_q \cdot \lambda_{p+q} \lambda_p^2](s_{12}, s_{23}) + s_{12}\, \mathcal{I}_4^{\text{bow-tie}}[\lambda_p \cdot \lambda_q](s_{12}) \Big\}\,,$$

$$A_{M1234}^{\text{P}_2} = \rho\Big\{ s_{12}\, \mathcal{I}_4^{\text{P}}[\lambda_p \cdot \lambda_q \lambda_{p+q}^2 - \lambda_p \cdot \lambda_{p+q} \lambda_q^2](s_{12}, s_{23}) + s_{12}\, \mathcal{I}_4^{\text{bow-tie}}[\lambda_p \cdot \lambda_q](s_{12}) \Big\}\,, \tag{6.14}$$

$$A_{M1234}^{\text{P}_3} = -\rho\Big\{ s_{12}\, \mathcal{I}_4^{\text{P}}[\lambda_p \cdot \lambda_{p+q} \lambda_q^2 + \lambda_q \cdot \lambda_{p+q} \lambda_p^2](s_{12}, s_{23}) + 4\, \mathcal{I}_4^{\text{bow-tie}}[\lambda_p^2 \lambda_q^2](s_{12}) \Big\}\,,$$

corresponding to the first three diagrams in fig. 8. For the case where the fermion and scalar loops are separated from each other, which does not contribute in the superpotential case, we have

$$A_{M1234}^{\text{P}_4} = -2\rho\Big\{ \mathcal{I}_4^{\text{bow-tie}}[\lambda_p \cdot \lambda_q(\lambda_p^2 + \lambda_q^2)](s_{12}) + \frac{4}{s_{12}} \mathcal{I}_4^{\text{bow-tie}}\Big[\lambda_p^2 \lambda_q^2((p+q)^2 + \tfrac{1}{2}s_{12})\Big](s_{12}, s_{23}) \Big\}\,. \tag{6.15}$$

The mixed contributions corresponding to the three non-planar parent diagrams in fig. 8 are

$$A_{M1234}^{\text{NP}_1} = \rho\, s_{12}\, \mathcal{I}_4^{\text{NP}}[\lambda_p \cdot \lambda_q \lambda_{p+q}^2 - \lambda_q \cdot \lambda_{p+q} \lambda_p^2](s_{12}, s_{23})\,,$$

$$A_{M1234}^{\text{NP}_2} = \rho\, s_{12}\, \mathcal{I}_4^{\text{NP}}[\lambda_p \cdot \lambda_q \lambda_{p+q}^2 - \lambda_p \cdot \lambda_{p+q} \lambda_q^2](s_{12}, s_{23})\,, \tag{6.16}$$

$$A_{M1234}^{\text{NP}_3} = -\rho\, s_{12}\, \mathcal{I}_4^{\text{NP}}[\lambda_p \cdot \lambda_{p+q} \lambda_q^2 + \lambda_q \cdot \lambda_{p+q} \lambda_p^2](s_{12}, s_{23})\,.$$

27

As in the previous cases, in the double box integrals we can label the numerator momentum factors in terms of which types of particles carry the loop momenta, *i.e.*,

$$-\lambda_{f_1} \cdot \lambda_{f_2} \lambda_s^2 \,. \tag{6.17}$$

In this case there are two contributions to each primitive amplitude above, since interchanging matter fermions with scalars in fig. 8 does not alter the color factor.

6.5 Amplitudes with both a gluino and matter loop

Up to color factors, the parent diagrams with both a gluino and matter loop depicted in figs. 9 and 10 are identical to the parent diagrams in fig. 6(P_4) and fig. 8(P_4). Thus, the associated primitive amplitudes are also simply related,

$$
\begin{aligned}
A_{\tilde{F}1234}^{P_1} &= A_{\tilde{F}1234}^{P_2} = A_{F1234}^{P_4} \,, \\
A_{\tilde{S}1234}^{P_1} &= -2\rho \left\{ \mathcal{I}_4^{\text{bow-tie}}[\lambda_p \cdot \lambda_q \lambda_q^2](s_{12}) + \frac{2}{s_{12}} \mathcal{I}_4^{\text{bow-tie}} \left[\lambda_p^2 \lambda_q^2 ((p+q)^2 + \tfrac{1}{2}s_{12}) \right] (s_{12}, s_{23}) \right\} , \\
A_{\tilde{S}1234}^{P_2} &= -2\rho \left\{ \mathcal{I}_4^{\text{bow-tie}}[\lambda_p \cdot \lambda_q \lambda_p^2](s_{12}) + \frac{2}{s_{12}} \mathcal{I}_4^{\text{bow-tie}} \left[\lambda_p^2 \lambda_q^2 ((p+q)^2 + \tfrac{1}{2}s_{12}) \right] (s_{12}, s_{23}) \right\} .
\end{aligned}
\tag{6.18}
$$

Hence

$$A_{\tilde{S}1234}^{P_1} + A_{\tilde{S}1234}^{P_2} = A_{M1234}^{P_4} \,, \tag{6.19}$$

accounting for the fact that $A_{M1234}^{P_4}$ incorporates the cases were the scalar loop is on the left or right in diagram (P_4) of fig. 8, while the diagrams in fig. 10 separate the two cases.

7 Two-loop supersymmetry identities

We now verify that the supersymmetry Ward identity (2.3) does in fact hold for the amplitudes presented in sect. 6 when using the FDH scheme.

7.1 $N = 1$ Identities

The two-loop $N = 1$ SWI are obtained by applying eq. (2.3) to eqs. (5.23) and (5.25). For convenience, we subdivide the SWI according to the independent parameters appearing in the amplitudes, n_f and ξ,

$$\mathcal{A}_G^{\text{adjoint}} + \mathcal{A}_F^{\text{adjoint}} = 0 \,, \tag{7.1}$$

$$\mathcal{A}_F^{\text{fund}(1)} + \mathcal{A}_S^{\text{fund}(1)} + \mathcal{A}_M^{\text{fund}(1)} + \mathcal{A}_{\tilde{F}}^{\text{fund}(1)} + \mathcal{A}_{\tilde{S}}^{\text{fund}(1)} = 0 \,, \tag{7.2}$$

$$\mathcal{A}_F^{\text{fund}(2)} + \mathcal{A}_S^{\text{fund}(2)} + \mathcal{A}_M^{\text{fund}(2)} = 0 \,, \tag{7.3}$$

$$\mathcal{A}_S^{\text{Yukawa}} + \mathcal{A}_M^{\text{Yukawa}} = 0 \,, \tag{7.4}$$

corresponding to the four sets of diagrams represented in fig. 2. These identities must hold if supersymmetry is preserved by a regularization scheme.

In general, we can further subdivide the identities by considering separately the coefficient of each linearly independent color factor. It turns out, however, that for the identical-helicity amplitude a slightly stronger subdivision is possible directly in terms of the primitive amplitudes presented in sect. 6. In other words, we shall show that the identities hold for each coefficient of the different color factors appearing in eqs. (5.14) and (5.20), even though they are not all linearly independent.

The following two integrals, which will appear on the right-hand-side of several of the identities, have a simple representation in terms of double-box integrals evaluated in $6 - 2\epsilon$ dimensions,

$$
\begin{aligned}
\mathcal{R}^{\mathrm{P}} &\equiv \rho\, s_{12}\, \mathcal{I}_4^{\mathrm{P}}\Big[(\lambda_p \cdot \lambda_q)^2 - \lambda_p^2 \lambda_q^2\Big](s_{12}, s_{23}) = -\frac{\epsilon}{2}(1 + 2\epsilon)\,(4\pi)^2\, \rho\, s_{12}\, \mathcal{I}_4^{\mathrm{P}, D=6-2\epsilon}(s_{12}, s_{23})\,, \\
\mathcal{R}^{\mathrm{NP}} &\equiv \rho\, s_{12}\, \mathcal{I}_4^{\mathrm{NP}}\Big[(\lambda_p \cdot \lambda_q)^2 - \lambda_p^2 \lambda_q^2\Big](s_{12}, s_{23}) = -\frac{\epsilon}{2}(1 + 2\epsilon)\,(4\pi)^2\, \rho\, s_{12}\, \mathcal{I}_4^{\mathrm{NP}, D=6-2\epsilon}(s_{12}, s_{23})\,,
\end{aligned}
\tag{7.5}
$$

where

$$
\begin{aligned}
&\mathcal{I}_4^{\mathrm{P}, D=6-2\epsilon}(s_{12}, s_{23}) \\
&\equiv \int \frac{d^{6-2\epsilon}p}{(2\pi)^{6-2\epsilon}} \frac{d^{6-2\epsilon}q}{(2\pi)^{6-2\epsilon}} \frac{1}{p^2\, q^2\, (p+q)^2 (p-k_1)^2\, (p-k_1-k_2)^2\, (q-k_4)^2\, (q-k_3-k_4)^2}\,, \\
&\mathcal{I}_4^{\mathrm{NP}, D=6-2\epsilon}(s_{12}, s_{23}) \\
&\equiv \int \frac{d^{6-2\epsilon}p}{(2\pi)^{6-2\epsilon}} \frac{d^{6-2\epsilon}q}{(2\pi)^{6-2\epsilon}} \frac{1}{p^2\, q^2\, (p+q)^2\, (p-k_1)^2\, (q-k_2)^2\, (p+q+k_3)^2\, (p+q+k_3+k_4)^2}\,.
\end{aligned}
\tag{7.6}
$$

The planar and non-planar double box integrals have neither infrared nor ultraviolet divergences in six dimensions. Therefore, due to the explicit ϵ in front of the integrals in eqs. (7.5), $\mathcal{R}^{\mathrm{P}}$ and $\mathcal{R}^{\mathrm{NP}}$ are both of $\mathcal{O}(\epsilon)$ as $\epsilon \to 0$.

We begin our inspection of the supersymmetry identities with eq. (7.1). This identity holds in the FDH scheme ($D_s = 4$), because the combinations

$$
A_{G1234}^{\mathrm{P}} + \sum_{i=1}^{4} A_{F1234}^{\mathrm{P}_i} = 6\,\mathcal{R}^{\mathrm{P}} = \mathcal{O}(\epsilon)\,,
\tag{7.7}
$$

$$
A_{G1234}^{\mathrm{NP}} + \sum_{i=1}^{3} A_{F1234}^{\mathrm{NP}_i} = 6\,\mathcal{R}^{\mathrm{NP}} = \mathcal{O}(\epsilon)\,,
\tag{7.8}
$$

vanish as $\epsilon \to 0$. The right-hand sides in these equations are obtained by inserting the explicit values of the primitive amplitudes given in sect. 6. We dropped the integrals that vanish identically, *i.e.* the bow-tie integrals that are odd in λ_p or λ_q. The same equations (7.7) and (7.8) obviously also hold after performing any permutation of the external legs.

Similarly, the identity (7.2) holds because

$$
\sum_{i=1}^{2}\Big(A_{F1234}^{\mathrm{P}_i} + A_{S1234}^{\mathrm{P}_i} + A_{M1234}^{\mathrm{P}_i}\Big) = -4\,\mathcal{R}^{\mathrm{P}} = \mathcal{O}(\epsilon)\,,
\tag{7.9}
$$

$$
A_{F1234}^{\mathrm{P}_3} + \sum_{i\in\{3,5\}} A_{S1234}^{\mathrm{P}_i} + A_{M1234}^{\mathrm{P}_3} = -2\,\mathcal{R}^{\mathrm{P}} = \mathcal{O}(\epsilon)\,,
\tag{7.10}
$$

$$
\sum_{i=1}^{2}\Big(A_{F1234}^{\mathrm{NP}_i} + A_{S1234}^{\mathrm{NP}_i} + A_{M1234}^{\mathrm{NP}_i}\Big) = -4\,\mathcal{R}^{\mathrm{NP}} = \mathcal{O}(\epsilon)\,,
\tag{7.11}
$$

29

$$A^{\mathrm{NP}_3}_{F1234} + A^{\mathrm{NP}_3}_{S1234} + A^{\mathrm{NP}_3}_{M1234} = -2\,\mathcal{R}^{\mathrm{NP}} = \mathcal{O}(\epsilon)\,, \tag{7.12}$$

$$A^{\mathrm{P}_1}_{\tilde{S}1234} + A^{\mathrm{P}_1}_{\tilde{F}1234} = A^{\mathrm{P}_2}_{\tilde{S}1234} + A^{\mathrm{P}_2}_{\tilde{F}1234} = 0\,, \tag{7.13}$$

and the identity (7.3) holds because

$$A^{P_4}_{F1234} - A^{P_4}_{S1234} = 0\,, \tag{7.14}$$

$$2\,A^{P_4}_{F1234} + A^{P_4}_{M1234} = 0\,. \tag{7.15}$$

The latter two equations hold to all orders in ϵ.

Finally, eq. (7.4), the identity for the amplitudes depending on the Yukawa coupling ξ, holds because

$$\frac{1}{2}\sum_{i=1}^{3} A^{\mathrm{P}_i}_{M1234} + 2A^{\mathrm{P}_5}_{S1234} = 2\,\mathcal{R}^{\mathrm{P}} = \mathcal{O}(\epsilon)\,, \tag{7.16}$$

$$\frac{1}{2}\sum_{i=1}^{3} A^{\mathrm{NP}_i}_{M1234} = 2\,\mathcal{R}^{\mathrm{NP}} = \mathcal{O}(\epsilon)\,, \tag{7.17}$$

where the factors of $1/2$ and 2 on the left-hand side of the equations are relative combinatoric factors compared to the gauge case.

The same relations hold for any permutation of the external legs. We conclude that for $D_s = 4$ (FDH scheme) the identical-helicity $(++++)$ primitive amplitudes satisfy the SWI (2.3) as $\epsilon \to 0$, at least through two loops. In the course of computing the two-loop amplitude for the helicity configuration $-+++$ in QCD [19], we have also verified that the pure super-Yang-Mills identity (7.1) is satisfied for $-+++$ up to $\mathcal{O}(\epsilon)$ corrections, again provided that $D_s = 4$. For either of these two helicity amplitudes, in the HV scheme where $D_s = 4 - 2\epsilon$ the identities (7.7) and (7.8) with gluon loops are *not* satisfied, even at $\mathcal{O}(\epsilon^{-1})$.

Even in the FDH scheme, the above two-loop $N = 1$ identities are generally satisfied only for $\epsilon \to 0$, because the quantities $\mathcal{R}^{\mathrm{P}}$ and $\mathcal{R}^{\mathrm{NP}}$ are known at order ϵ, and they are nonvanishing at this order. If one thinks about constructing three-loop amplitudes via their unitarity cuts, including the two-loop $\times$ tree cuts, one might be concerned that the $\mathcal{O}(\epsilon)$ breaking of the identities at two loops could lead to a non-vanishing breaking of the SWI at three loops even as $\epsilon \to 0$. Of course there will also be contributions to the two-loop $\times$ tree cuts from intermediate momenta in (-2ϵ) dimensions, which may well cancel the above contributions. Clearly this issue warrants further investigation.

7.2 Exactness of $N = 2$ Identities

An $\mathcal{O}(\epsilon)$ breaking in $N = 1$ supersymmetry Ward identities in the FDH scheme is perhaps to be expected since the scheme is defined by "dimensional expansion", *i.e.*, $D > 4$. Supermultiplets become larger as D increases; hence for $D > 4$ an $N = 1$ supersymmetric theory in $D = 4$ does not provide enough states to form a supermultiplet for the intermediate unobserved states with momenta in the extra (-2ϵ) dimensions. Thus, one might expect some kind of violation of supersymmetry for finite ϵ. On the other hand, the $N = 2$ vector multiplet, consisting of a gluon, two gluinos and a complex scalar, may be viewed as coming from the compactification of a higher-dimensional

supersymmetric theory, for example $N = 1$ supersymmetric gauge theory in $D = 5$. So, under a dimensional expansion of the $N = 2$ theory away from $D = 4$ there are sufficiently many states to form a supermultiplet, and we might expect the SWI to hold to all orders in ϵ in the $N = 2$ case. The supersymmetry identity that should be satisfied in pure $N = 2$ gauge theory is given in eq. (5.27). This identity does hold to all orders in ϵ, because of the following relations between primitive amplitudes:

$$A_{G1234}^{\mathrm{P}} + \sum_{i=1}^{5} A_{S1234}^{\mathrm{P}i} + \sum_{i=1}^{3}(2A_{F1234}^{\mathrm{P}i} + A_{M1234}^{\mathrm{P}i}) + 4A_{F1234}^{\mathrm{P}4} + 2A_{M1234}^{\mathrm{P}4} = 0\,, \tag{7.18}$$

which is the sum of eqs. (7.7), (7.9), and (7.10); and

$$A_{G1234}^{\mathrm{NP}} + \sum_{i=1}^{3}(A_{S1234}^{\mathrm{NP}i} + 2A_{F1234}^{\mathrm{NP}i} + A_{M1234}^{\mathrm{NP}i}) = 0\,, \tag{7.19}$$

which is the sum of eqs. (7.8), (7.11), and (7.12).

Now consider adding n_f hypermultiplets in the $N_c + \bar{N}_c$ representation to the $N = 2$ gauge theory. The $N = 2$ hypermultiplets have the same field content as the pairs of $N = 1$ chiral matter fields, $Q_i + \tilde{Q}_i$. The n_f^2 terms in the SWI for $D_s = 4$ clearly hold to all orders in ϵ, by virtue of eqs. (7.14) and (7.15). The same statement is true for the n_f^1 terms, however here the cancellation is more subtle. One can split the $N = 2$ gauge multiplet into an $N = 1$ gauge multiplet plus an $N = 1$ adjoint matter multiplet Φ. There is a set of n_f^1 contributions from coupling the hypermultiplet fields to the $N = 1$ gauge fields, which is given by precisely the combinations (7.9)–(7.12) encountered above. A second set of n_f^1 contributions comes from coupling the hypermultiplet fields to Φ. This coupling is through an $N = 1$ superpotential term, $\tilde{W} \propto \sum_i \tilde{Q}_i \Phi Q_i$. The strength of $\tilde{W}$ is dictated by the gauge coupling, because the Yukawa interactions with the $N = 1$ gaugino λ in eq. (2.5) have to be duplicated by couplings to the $N = 1$ matter adjoint fermion, which is the second gaugino of $N = 2$ supersymmetry. These Yukawa interactions just double the mixed fermion-scalar terms, $A_{M1234}^{\mathrm{P}i}$ and $A_{M1234}^{\mathrm{NP}i}$. However, there are additional mixed terms due to the Yukawa vertices from $\tilde{W}$ which contain the adjoint scalar particle. These terms are dressed a bit differently with color than the mixed contributions considered in sect. 5.3. However, they still can be written in terms of $A_{M1234}^{\mathrm{P}i}$ and $A_{M1234}^{\mathrm{NP}i}$. Finally, there are new P_5 terms from scalar four-point interactions generated by $\tilde{W}$. Adding all the terms together, we find that the SWI hold to all orders in ϵ by virtue of

$$\sum_{i=1}^{2}\left(A_{F1234}^{\mathrm{P}i} + A_{S1234}^{\mathrm{P}i} + A_{M1234}^{\mathrm{P}i}\right) + \left(\sum_{i=1}^{3} A_{M1234}^{\mathrm{P}i} + 4A_{S1234}^{\mathrm{P}5}\right) = 0\,, \tag{7.20}$$

$$\left(A_{F1234}^{\mathrm{P}3} + \sum_{i\in\{3,5\}} A_{S1234}^{\mathrm{P}i} + A_{M1234}^{\mathrm{P}3}\right) + \frac{1}{2}\left(\sum_{i=1}^{3} A_{M1234}^{\mathrm{P}i} + 4A_{S1234}^{\mathrm{P}5}\right) = 0\,, \tag{7.21}$$

$$\sum_{i=1}^{2}\left(A_{F1234}^{\mathrm{NP}i} + A_{S1234}^{\mathrm{NP}i} + A_{M1234}^{\mathrm{NP}i}\right) + \left(\sum_{i=1}^{3} A_{M1234}^{\mathrm{NP}i}\right) = 0\,, \tag{7.22}$$

$$\left(A_{F1234}^{\mathrm{NP}3} + A_{S1234}^{\mathrm{NP}3} + A_{M1234}^{\mathrm{NP}3}\right) + \frac{1}{2}\left(\sum_{i=1}^{3} A_{M1234}^{\mathrm{NP}i}\right) = 0\,, \tag{7.23}$$

which follow from adding appropriate pairs of eqs. (7.9)–(7.17).

8 Renormalization

The identical-helicity amplitudes presented in sect. 6 have not been renormalized. Since the corresponding tree-level amplitudes vanish for this helicity configuration, the renormalization procedure is similar to that for a typical one-loop amplitude. In particular, the modified minimal subtraction counterterm to be subtracted from $\mathcal{A}_4^{\text{2-loop}}(1^+, 2^+, 3^+, 4^+)$ is

$$\text{C.T.} = 4g^2 b_0 \, c_\Gamma \, \frac{1}{\epsilon} \, \mathcal{A}_4^{\text{1-loop}}(1^+, 2^+, 3^+, 4^+) \,, \tag{8.1}$$

where

$$c_\Gamma \equiv \frac{\Gamma(1+\epsilon)\Gamma^2(1-\epsilon)}{\Gamma(1-2\epsilon)(4\pi)^{2-\epsilon}} \,, \tag{8.2}$$

and b_0 is the one-loop β-function coefficient. For example, in QCD with N_c colors and n_f quark flavors,

$$b_0^{\text{QCD}} = \frac{11N_c - 2n_f}{6} \,, \tag{8.3}$$

while for pure $N = 1$ super-Yang-Mills theory,

$$b_0^{N=1} = \frac{3}{2} N_c \,. \tag{8.4}$$

More generally, the counterterms depend on the scheme choice through the scheme dependence of the one-loop amplitude.

8.1 Coupling constant shift

When comparing physical results obtained in the FDH scheme to ones obtained in the 't Hooft-Veltman (HV) scheme, one must account for the shift in the coupling. In general, the coupling constant of the theory is scheme dependent. The one-loop relation between the QCD coupling constant in dimensional regularization and that in dimensional reduction has been computed previously [8, 31, 32, 11]. Here we shall give the relation to two loops. We also allow for an arbitrary value of the variable controlling the number of gluon states in loops, $D_s \equiv 4 - 2\epsilon\delta_R$, so that one can consider schemes other than the FDH/$\overline{\text{DR}}$ scheme ($\delta_R = 0$) or the HV scheme ($\delta_R = 1$) if one desires.

A convenient method for calculating the scheme dependence of the coupling constant is to evaluate the shift in the background field gauge method [51, 52, 53, 54] by computing the vacuum polarization, following the one-loop discussion of ref. [11]. The background field gauge possesses a Ward identity $Z_g = Z_A^{-1/2}$ which allows one to obtain the coupling constant renormalization Z_g from the wave-function renormalization Z_A. Our two-loop computation follows closely the ones in refs. [52, 53], except that we have to keep track of the finite terms, not just the poles in ϵ, when the terms are scheme dependent.

The coupling constants of the 't Hooft-Veltman and CDR schemes are identical because the vacuum polarizations are computed using exactly the same rules for internal states. The HV and CDR regularization schemes, together with the widely used modified minimal subtraction ($\overline{\text{MS}}$) renormalization scheme, define the coupling constant $\alpha_{\overline{\text{MS}}}$. The modified minimally subtracted

versions of the FDH and DR schemes, which we call $\overline{\text{FDH}}$ and $\overline{\text{DR}}$, define the coupling constant $\alpha_{\overline{\text{FDH}}} = \alpha_{\overline{\text{DR}}}$. For any coupling α, let the reduced coupling be $a = \alpha/(2\pi)$. Then the one-loop coupling constant relation is [8, 31, 32, 11]

$$a_{\overline{\text{DR}}} = a_{\overline{\text{FDH}}} = a_{\overline{\text{MS}}}\left(1 + \frac{C_A}{6}a_{\overline{\text{MS}}} + \cdots\right),$$

where C_A is the quadratic Casimir in the adjoint representation, $C_A = N_c$ for gauge group $SU(N_c)$. Our goal here is to compute the two-loop corrections to this relation.

A priori, there is a difference between FDH and DR, in that DR divides a gluon Lorentz index into a $D = 4 - 2\epsilon$ index and a residual 2ϵ index. The latter components are referred to as ϵ-scalars. Imposing D-dimensional gauge invariance still permits the ϵ-scalars, and their associated couplings, to renormalize differently from the D-dimensional gauge fields. For example, when fermions are present, their coupling g to the gauge fields gives rise to a Yukawa coupling $\hat{g}$ of the fermions to the ϵ-scalars. In a non-supersymmetric theory, when one also requires the ϵ-scalar Green functions to be finite, one finds that g and $\hat{g}$ have different β functions even at one loop [9].

A nice feature of the background field method is that none of the quantum fields have to be renormalized [52]. Quantum fields do not appear on the external (background) legs, so Z factors cancel between propagators and vertices. Therefore, one does not have to worry in the present calculation about whether the ϵ-scalars that are present in DR should be renormalized differently from the d-dimensional gauge fields. Thus, the counterterm graphs are identical between DR and FDH. The non-counterterm graphs also turn out to be identical; the D and 2ϵ ranges of the indices in DR combine to give exactly the four-dimensional range used in FDH. Thus the $\overline{\text{FDH}}$ and $\overline{\text{DR}}$ gauge couplings are equivalent, at least in any theory (supersymmetric or not) with only a gauge coupling present.

Following the computational rules for the FDH scheme, we write the Lorentz contraction that tracks the number of physical states as

$$\eta^\mu_\mu = D_s = 4 - 2\epsilon\,\delta_R\,, \tag{8.5}$$

where η is the Minkowski metric, $\delta_R = 1$ for $\overline{\text{MS}}$, $\delta_R = 0$ for $\overline{\text{DR}}$ or $\overline{\text{FDH}}$. In ref. [52, 53] the divergent terms in the two-loop vacuum polarization were computed in $\overline{\text{MS}}$. Here we also need the portion of the finite terms that depends on δ_R. For pure gauge theory, Table 1 of ref. [52] gives the divergent parts of the Feynman graphs shown in fig. 12. Of the graphs a–m, only b, h, k, and the counterterm graphs l and m, are δ_R dependent, although a little inspection is necessary to show that graphs d and e are independent of δ_R.

The counterterm contributions l and m come from one-loop renormalization of the gauge-fixing terms. For our purposes, this renormalization has to be performed including the finite level, whereas in obtaining the β function in ref. [52] it was sufficient to carry out the renormalization only through $\mathcal{O}(1/\epsilon)$. We find that the gauge-fixing renormalization factor Z_α is given by

$$Z_\alpha = 1 + \left[\left(\frac{5}{3\epsilon} + \frac{\delta_R}{3} + \frac{28}{9}\right)C_A - \left(\frac{4}{3\epsilon} + \frac{20}{9}\right)T_F\right]\frac{g^2}{(4\pi)^2}\,, \tag{8.6}$$

where the fermion generators have trace $\text{Tr}(T^aT^b) = T_F\delta^{ab}$ (for QCD with n_f flavors, $T_F = \frac{1}{2}n_f$).
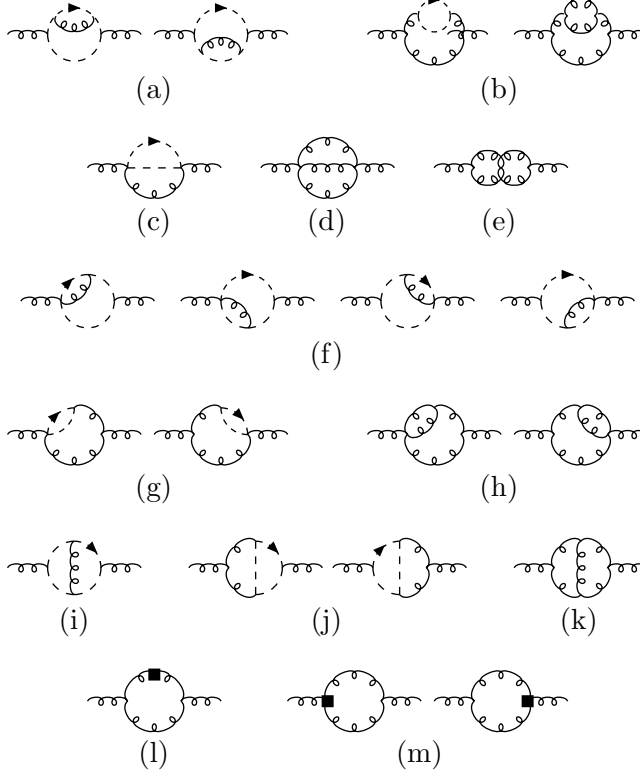
33

Figure 12: Feynman diagrams for the pure glue contributions to the vacuum polarization, following the labeling of ref. [52]. Dashed lines represent ghosts, and square dots represent counterterms.

In the notation of refs. [52, 53], the vacuum polarization is

$$\Pi_{\mu\nu}(k) = \frac{ig^4 C_A^2 \delta^{ab}}{(4\pi)^4} \left[A g_{\mu\nu} - B k_\mu k_\nu \right]. \tag{8.7}$$

In the background field method the final sum over diagrams gives $A = B$, ensuring the transversality of the vacuum polarization. Here we give just the B terms, dropping for convenience the combination $\gamma_E - \ln 4\pi + \ln(k^2/\mu^2)$, as well as all δ_R-independent finite contributions. For the B terms of eq. (8.7) we obtain,

$$
\begin{aligned}
\text{graph b:} \quad & \frac{25}{6\epsilon^2}\left(1 + \frac{22}{5}\epsilon\right) + \frac{3}{2\epsilon}(\delta_R - 1) + \frac{49}{6}\delta_R, \\
\text{graph h:} \quad & -\frac{9}{8\epsilon^2}\left(1 + \frac{31}{6}\epsilon\right) - \frac{3}{4\epsilon}(\delta_R - 1) - \frac{27}{8}\delta_R, \\
\text{graph k:} \quad & \frac{27}{8\epsilon^2}\left(1 + \frac{245}{54}\epsilon\right) - \frac{3}{4\epsilon}(\delta_R - 1) - \frac{25}{8}\delta_R, \\
\text{graphs l+m:} \quad & \frac{10}{3\epsilon} + \frac{2}{3}\delta_R, \\
\text{a–m total:} \quad & \frac{17}{3\epsilon} + \frac{7}{3}\delta_R.
\end{aligned}
\tag{8.8}
$$

The values of the remaining graphs with no δ_R dependence may be obtained from ref. [52].

For the fermion-loop contributions shown in fig. 13, we find that the only finite δ_R-dependent
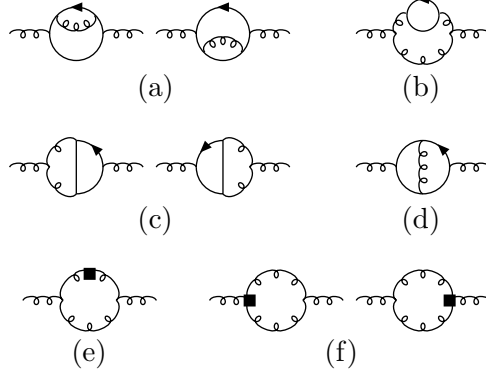
34

Figure 13: Fermion loop contributions to the vacuum polarization, following ref. [53]. Solid lines represent fermions, and square dots represent counterterms.

terms that survive are in the $T_F C_F$ color structure, and the total in Table 1 from ref. [53] becomes

$$\text{total:} \qquad -\frac{1}{\epsilon}\Big(\frac{10}{3}T_F C_A + 2T_F C_F\Big) - 2T_F C_F \delta_R\,. \qquad (8.9)$$

Here C_F is the quadratic Casimir in the fermion representation, $C_F = (N_c^2 - 1)/(2N_c)$ for the fundamental representation of $SU(N_c)$. It is rather simple to see that adding scalars to the theory does not induce any additional δ_R dependence; the corresponding diagrams do not contain any η^μ_μ contractions.

The background field Ward identity [52] relates the inverse coupling directly to the vacuum polarization. Using this relation, we find that the bare inverse coupling is given in terms of the renormalized coupling $a_{\delta_R} \equiv \alpha_{\delta_R}/(2\pi)$ by

$$\frac{1}{a_{\text{bare}}} = \frac{1}{a_{\delta_R}}\bigg\{ 1 - a_{\delta_R}\Big[\frac{1}{2\epsilon}\Big(\frac{11}{3}C_A - \frac{4}{3}T_F\Big) + \frac{1}{6}C_A\delta_R + c_1\Big]\Big(\frac{e^{\gamma_E}k^2}{4\pi}\Big)^{-\epsilon}$$
$$- a_{\delta_R}^2\Big[\frac{1}{8\epsilon}\Big(\frac{34}{3}C_A^2 - \frac{20}{3}T_F C_A - 4T_F C_F\Big) + \Big(\frac{7}{12}C_A^2 - \frac{1}{2}T_F C_F\Big)\delta_R + c_2\Big]\Big(\frac{e^{\gamma_E}k^2}{4\pi}\Big)^{-2\epsilon}\bigg\}\,, \qquad (8.10)$$

where c_1 and c_2 are independent of δ_R. To relate a_{δ_R} to the standard $\overline{\text{MS}}$ coupling, $a \equiv \alpha_{\overline{\text{MS}}}/(2\pi)$ with $\delta_R = 1$, we equate the two versions of the bare inverse coupling, which leads to

$$a_{\delta_R} = a\bigg[1 + \frac{1}{6}C_A(1 - \delta_R)\,a + \Big(\frac{7}{12}C_A^2(1 - \delta_R) + \frac{1}{36}C_A^2(1 - \delta_R)^2 - \frac{1}{2}T_F C_F(1 - \delta_R)\Big)a^2\bigg]\,. \qquad (8.11)$$

In particular, for a gauge theory with a general fermion content, the $\overline{\text{DR}}$ coupling, $\tilde{a} \equiv \alpha_{\overline{\text{DR}}}/(2\pi)$, is expressed in terms of the $\overline{\text{MS}}$ coupling by setting $\delta_R = 0$ in eq. (8.11), yielding

$$\tilde{a} = a\bigg[1 + \frac{1}{6}C_A\,a + \Big(\frac{11}{18}C_A^2 - \frac{1}{2}T_F C_F\Big)a^2\bigg] + \mathcal{O}(a^3)\,. \qquad (8.12)$$

8.2 Three-loop β function

An interesting side-benefit of the above computation is that it allows us to obtain the *three*-loop β function in the $\overline{\text{FDH}}$ and $\overline{\text{DR}}$ schemes from the known β function in the $\overline{\text{MS}}$ scheme [33].

In general, knowledge of the scheme dependence of the coupling allows one to convert the β function between schemes at one higher loop order. For example, the β-function coefficients in four different momentum-subtraction (MOM) schemes were computed at *four* loops in similar fashion [55]; see also refs. [56] for three-loop MOM computations. There are similar computations on the lattice [57].

Consider two different renormalization schemes, and hence two different coupling constants, for a single theory,

$$a \equiv \frac{\alpha}{2\pi}, \qquad \tilde{a} \equiv \frac{\tilde{\alpha}}{2\pi}, \tag{8.13}$$

and suppose they are related through two loops by

$$
\begin{aligned}
\tilde{a} &= a\Big[1 + d_1 a + d_2 a^2 + \ldots\Big], \\
a &= \tilde{a}\Big[1 - d_1 \tilde{a} + (2d_1^2 - d_2)\tilde{a}^2 + \ldots\Big].
\end{aligned}
\tag{8.14}
$$

Let the β functions in the two schemes be

$$
\begin{aligned}
\mu\frac{da}{d\mu} &\equiv \beta(a) \equiv -2\Big[b_0 a^2 + b_1 a^3 + b_2 a^4 + \ldots\Big], \\
\mu\frac{d\tilde{a}}{d\mu} &\equiv \tilde{\beta}(\tilde{a}) \equiv -2\Big[\tilde{b}_0 \tilde{a}^2 + \tilde{b}_1 \tilde{a}^3 + \tilde{b}_2 \tilde{a}^4 + \ldots\Big].
\end{aligned}
\tag{8.15}
$$

One can also calculate the β function in the second scheme as

$$\tilde{\beta}(\tilde{a}) = \mu\frac{d\tilde{a}}{d\mu} = \mu\frac{da}{d\mu} \times \frac{d\tilde{a}}{da} = \beta(a) \times [1 + 2d_1 a + 3d_2 a^2 + \ldots]. \tag{8.16}$$

Comparing this expression with that in eq. (8.15), after substituting for $\tilde{a}$ using eq. (8.14), we have

$$
\begin{aligned}
&[b_0 a^2 + b_1 a^3 + b_2 a^4 + \ldots] \times [1 + 2d_1 a + 3d_2 a^2 + \ldots] \\
&= \tilde{b}_0 a^2[1 + d_1 a + d_2 a^2 + \ldots]^2 + \tilde{b}_1 a^3[1 + d_1 a + \ldots]^3 + \tilde{b}_2 a^4[1 + \ldots]^4
\end{aligned}
\tag{8.17}
$$

Equating coefficients of a gives the standard results that $\tilde{b}_0 = b_0$ and $\tilde{b}_1 = b_1$, and also

$$\tilde{b}_2 = b_2 - d_1^2 b_0 - d_1 b_1 + d_2 b_0. \tag{8.18}$$

This gives the shift in the three-loop β-function coefficient in terms of the one- and two-loop coupling constant shifts d_1 and d_2.

To compute the three-loop β-function coefficient in $\overline{\text{DR}}$ scheme, we now use eq. (8.18), in conjunction with the well-known three-loop β function in $\overline{\text{MS}}$ [58, 59, 33, 54],

$$
\begin{aligned}
b_0 &= \frac{11}{6}C_A - \frac{2}{3}T_F, \\
b_1 &= \frac{17}{6}C_A^2 - \frac{5}{3}C_A T_F - C_F T_F, \\
b_2 &= \frac{2857}{432}C_A^3 - \frac{1415}{216}C_A^2 T_F - \frac{205}{72}C_A C_F T_F + \frac{1}{4}C_F^2 T_F + \frac{79}{108}C_A T_F^2 + \frac{11}{18}C_F T_F^2.
\end{aligned}
\tag{8.19}
$$

Hence the three-loop β-function coefficient in $\overline{\text{DR}}$ is

$$\tilde{b}_2 = \frac{3115}{432}C_A^3 - \frac{1439}{216}C_A^2 T_F - \frac{259}{72}C_A C_F T_F + \frac{1}{4}C_F^2 T_F + \frac{79}{108}C_A T_F^2 + \frac{17}{18}C_F T_F^2. \tag{8.20}$$

36

For QCD, $SU(3)$ with n_f flavors of quarks, the result is

$$\tilde{b}_2 = \frac{3115}{16} - \frac{5321}{144}n_f + \frac{373}{432}n_f^2 \,. \tag{8.21}$$

For a generic number of flavors, this value is significantly closer to the $\overline{\text{MS}}$ value than are the MOM versions of b_2 reported in refs. [56, 55], although for five flavors the MOMggg value [56] happens to be the closest to $\overline{\text{MS}}$. The result (8.20) should be obtainable as an extension of the work of ref. [54]. In that paper, three-loop β functions were calculated for a variety of theories, in a way that could be applied to both $\overline{\text{MS}}$ and $\overline{\text{DR}}$ schemes, but only the $\overline{\text{MS}}$ results were presented.

For the special case of pure super-Yang-Mills theory, with a single Majorana gluino, we set $T_F = C_A/2$, $C_F = C_A$, to obtain

$$
\begin{aligned}
b_0 &= \frac{3}{2}C_A \,, & b_1 &= \frac{3}{2}C_A^2 \,, \\
b_2 &= \frac{19}{8}C_A^3 \,, & \tilde{b}_2 &= \frac{21}{8}C_A^3 \,,
\end{aligned}
\tag{8.22}
$$

in agreement with ref. [60]. (The $\overline{\text{MS}}$ value, b_2, was first calculated in ref. [33].)

8.3 Scheme dependence of the primitive amplitudes

Since our expressions for the amplitudes in sect. 6 smoothly interpolate between the FDH ($D_s = 4$) and HV ($D_s = 4 - 2\epsilon$) schemes we obtain the scheme dependence of the amplitudes by subtracting the two forms. First consider the pure glue amplitude. From eqs. (6.1) and (6.2), that the difference between the unrenormalized pure glue primitive amplitudes in the two schemes is:

$$
\begin{aligned}
\delta A_{G1234}^{\text{P}} \equiv A_{G1234}^{\text{P,FDH}} - A_{G1234}^{\text{P,HV}} &= -4\frac{c_\Gamma}{\epsilon}\left(\frac{\mu^2}{-s}\right)^\epsilon \frac{\rho}{i}\mathcal{I}_4^{\text{1-loop}}[\lambda_p^4] + \mathcal{O}(\epsilon) \\
&= -2\frac{c_\Gamma}{\epsilon}\left(\frac{\mu^2}{-s}\right)^\epsilon A_4^{\text{gluon loop,FDH}}(1_g^+, 2_g^+, 3_g^+, 4_g^+) + \mathcal{O}(\epsilon) \,,
\end{aligned}
\tag{8.23}
$$

where we used eq. (A.11) of ref. [15] to obtain the first line and eq. (5.10) to obtain the second. Similarly, for the non-planar pure glue primitive amplitudes

$$\delta A_{G1234}^{\text{NP}} \equiv A_{G1234}^{\text{NP,FDH}} - A_{G1234}^{\text{NP,HV}} = -\frac{c_\Gamma}{\epsilon}\left(\frac{\mu^2}{-s}\right)^\epsilon A_4^{\text{gluon loop,FDH}}(1_g^+, 2_g^+, 3_g^+, 4_g^+) + \mathcal{O}(\epsilon) \,, \tag{8.24}$$

where we used eq. (A.14) of ref. [15]. In these expressions, the coupling associated with the HV amplitude is the standard $\overline{\text{MS}}$ one, and the coupling associated with the FDH amplitude is the $\overline{\text{DR}}$ one. This shift does not include the coupling shift (8.11) or the shift in the counterterm, which are straightforward to incorporate. For the remaining cases with fermion, scalar, or mixed loops we find that the differences are all of $\mathcal{O}(\epsilon)$. For example,

$$
\begin{aligned}
\delta A_{F1234}^{\text{P}_1} &= -\epsilon\rho\left\{s_{12}\mathcal{I}_4^{\text{P}}[\lambda_p^2\lambda_q^2 + \lambda_p \cdot \lambda_q\lambda_q^2] + 2\mathcal{I}_4^{\text{bow-tie}}\left[\lambda_q^2\left(\lambda_p \cdot \lambda_q + \frac{2}{s_{12}}\lambda_p^2((p+q)^2 + s_{12})\right)\right]\right\} = \mathcal{O}(\epsilon) \,, \\
\delta A_{F1234}^{\text{NP}_1} &= -\epsilon\rho s_{12}\mathcal{I}_4^{\text{NP}}[\lambda_p^2\lambda_q^2 + \lambda_p \cdot \lambda_q\lambda_q^2] = \mathcal{O}(\epsilon) \,.
\end{aligned}
\tag{8.25}
$$

37

The simple structure of the primitive amplitude scheme shift is, of course, not accidental. It may be understood in terms of the infrared divergences [50] appearing in the amplitudes. As one shifts between the schemes the integrands undergo shifts of $\mathcal{O}(\epsilon)$. These shifts can contribute only when they are multiplied by ϵ^{-1} divergences. The complete scheme dependence through $\mathcal{O}(\epsilon^0)$ therefore depends only on the scheme dependence of the universal divergences. The scheme shift for two-loop helicity amplitudes for which the tree amplitudes vanish are especially simple, because the divergences are rather like those of typical one-loop amplitudes. One may also shift the amplitudes of sect. 6 to the CDR scheme following the same strategy used at one loop [11, 30]. For more general helicity amplitudes, the scheme shift is more complicated because one must account for non-trivial scheme dependence in the $\boldsymbol{I}^{(2)}(\epsilon, \mu^2; \{p\})$ function of Catani [50]. These issues are presented in more detail in ref. [19].

9   Conclusions

In this paper we presented detailed rules for the four-dimensional helicity (FDH) regularization scheme to higher loops. The scheme is designed to preserve the number of bosonic and fermionic states at their four-dimensional values. Computationally, it amounts to a relatively minor modification of the 't Hooft-Veltman [2] dimensional regularization scheme. As an initial check of the supersymmetric properties at higher loops, we explicitly evaluated a number of two-loop examples, illustrating that the scheme preserves the required supersymmetry Ward identities, while the 't Hooft-Veltman scheme fails (as expected) to do so. The identities checked in this paper were relatively simple to evaluate directly, because they involved identical-helicity four-gluon amplitudes which have an especially simple analytic structure. Although we did not present it here, we verified that for $N = 1$ super-Yang-Mills theory, the $-+++$ helicity amplitude [19] also vanishes in the FDH scheme, in accordance with supersymmetry. It would be interesting to systematically investigate the supersymmetric properties of the remaining helicity amplitudes. In these cases the Ward identities relate amplitudes with four external gluons to amplitudes with external fermions as well; the former have been computed [19] but the latter have not.

By keeping track of a parameter δ_R which smoothly interpolates between the 't Hooft-Veltman and four-dimensional helicity schemes, one can conveniently verify that supersymmetry Ward Identities hold even in non-supersymmetric theories such as QCD — after modifying color factors and multiplicities so that states fall into supermultiplets. This approach is of some interest in non-trivial QCD calculations, where it can serve as a cross check. Indeed, the fact that the two-loop identical-helicity amplitude presented here satisfies the required supersymmetry Ward identities provides one additional check on the four-gluon QCD amplitudes of refs. [18, 19]. We mention that the more complicated helicity amplitudes in ref. [19] were decomposed into supersymmetric and non-supersymmetric pieces. The FDH scheme was applied to the supersymmetric pieces in order to preserve their supersymmetry; the same functions will thus appear in a supersymmetric decomposition of the two-quark-two-gluon and four-quark amplitudes.

In this paper we also evaluated the two-loop relation between the standard $\overline{\text{MS}}$ coupling and the couplings in the four-dimensional helicity and dimensional reduction schemes. It turns out that

the couplings in the latter two schemes are identical, at least in the case of a single gauge coupling. The two-loop coupling shift was then used to obtain the three-loop gauge theory β function in the dimensional reduction and four-dimensional helicity schemes, using the previously calculated [58, 59, 33] $\overline{\text{MS}}$ β-function.

It would be interesting to investigate the supersymmetry-preserving properties of the FDH scheme more generally. In particular, some open issues are whether the FDH scheme continues to preserve supersymmetry beyond two loops, and whether there are any subtleties analogous to the evanescent couplings that appear in the dimensional reduction scheme.

References

[1] J.C. Collins, *Renormalization: an introduction to the renormalization group, and the operator-product expansion*, Cambridge Univ. Press, 1984 (Cambridge Monographs on Mathematical Physics).

[2] G. 't Hooft and M. Veltman, Nucl. Phys. **B44**, 189 (1972).

[3] F.A. Berends, R. Kleiss, P. De Causmaecker, R. Gastmans and T.T. Wu, Phys. Lett. B **103**, 124 (1981);
P. De Causmaecker, R. Gastmans, W. Troost and T.T. Wu, Phys. Lett. B **105**, 215 (1981);
R. Kleiss and W.J. Stirling, Nucl. Phys. B **262**, 235 (1985);
J.F. Gunion and Z. Kunszt, Phys. Lett. B **161**, 333 (1985);
Z. Xu, D. Zhang and L. Chang, Nucl. Phys. B **291**, 392 (1987).

[4] M.L. Mangano and S.J. Parke, Phys. Rept. **200**, 301 (1991);
L.J. Dixon, in *Proceedings of Theoretical Advanced Study Institute in Elementary Particle Physics (TASI 95)*, ed. D.E. Soper, World Scientific, 1996 [arXiv:hep-ph/9601359].

[5] Z. Bern and D.A. Kosower, Nucl. Phys. **B379**, 451 (1992).

[6] Z. Bern, L.J. Dixon and D.A. Kosower, Ann. Rev. Nucl. Part. Sci. **46**, 109 (1996) [arXiv:hep-ph/9602280].

[7] W. Siegel, Phys. Lett. **B84**, 193 (1979);
D. M. Capper, D.R.T. Jones and P. van Nieuwenhuizen, Nucl. Phys. **B167**, 479 (1980);
I. Jack, D.R.T. Jones and K.L. Roberts, Z. Phys. **C63**, 151 (1994) [arXiv:hep-ph/9401349].

[8] G. Altarelli, G. Curci, G. Martinelli and S. Petrarca, Nucl. Phys. B **187**, 461 (1981).

[9] I. Jack, D.R.T. Jones and K.L. Roberts, Z. Phys. C **62**, 161 (1994) [arXiv:hep-ph/9310301].

[10] V.A. Novikov, M.A. Shifman, A.I. Vainshtein and V.I. Zakharov, Nucl. Phys. B **229**, 407 (1983);
V.A. Novikov, M.A. Shifman, A.I. Vainshtein and V.I. Zakharov, Phys. Lett. B **166**, 329 (1986) [Sov. J. Nucl. Phys. **43**, 294 (1986); Yad. Fiz. **43**, 459 (1986)];
M.A. Shifman and A.I. Vainshtein, Nucl. Phys. B **277**, 456 (1986) [Sov. Phys. JETP **64**, 428 (1986)];
I. Jack, D.R.T. Jones and C.G. North, Nucl. Phys. B **486**, 479 (1997) [arXiv:hep-ph/9609325];
I. Jack, D.R.T. Jones and A. Pickering, Phys. Lett. B **435**, 61 (1998) [arXiv:hep-ph/9805482].

[11] Z. Kunszt, A. Signer and Z. Trócsányi, Nucl. Phys. **B411**, 397 (1994) [arXiv:hep-ph/9305239].

[12] M.T. Grisaru, H.N. Pendleton and P. van Nieuwenhuizen, Phys. Rev. **D15**, 996 (1977);
M.T. Grisaru and H.N. Pendleton, Nucl. Phys. **B124**, 81 (1977).

[13] S.J. Parke and T.R. Taylor, Phys. Lett. **B157**, 81 (1985), err. *ibid.* **B174**, 465 (1986).

[14] Z. Bern, J.S. Rozowsky and B. Yan, Phys. Lett. **B401**, 273 (1997) [arXiv:hep-ph/9702424];

[15] Z. Bern, L.J. Dixon and D.A. Kosower, JHEP **0001**, 027 (2000) [arXiv:hep-ph/0001001].

[16] Z. Bern, L.J. Dixon and A. Ghinculov, Phys. Rev. D **63**, 053007 (2001) [arXiv:hep-ph/0010075].

[17] C. Anastasiou, E.W.N. Glover, C. Oleari and M.E. Tejeda-Yeomans, Nucl. Phys. B **601**, 318 (2001) [arXiv:hep-ph/0010212]; Nucl. Phys. B **601**, 341 (2001) [arXiv:hep-ph/0011094]; Nucl. Phys. B **605**, 486 (2001) [arXiv:hep-ph/0101304].

[18] E.W.N. Glover, C. Oleari and M.E. Tejeda-Yeomans, Nucl. Phys. B **605**, 467 (2001) [arXiv:hep-ph/0102201].

[19] Z. Bern, A. De Freitas and L.J. Dixon, preprint arXiv:hep-ph/0201161.

[20] Z. Bern, A. De Freitas and L.J. Dixon, JHEP **0109**, 037 (2001) [arXiv:hep-ph/0109078].

[21] Z. Bern, A. De Freitas, L.J. Dixon, A. Ghinculov and H.L. Wong, JHEP **0111**, 031 (2001) [arXiv:hep-ph/0109079].

[22] V.A. Smirnov, Phys. Lett. **B460**, 397 (1999) [arXiv:hep-ph/9905323].

[23] J.B. Tausk, Phys. Lett. **B469**, 225 (1999) [arXiv:hep-ph/9909506].

[24] V.A. Smirnov and O.L. Veretin, Nucl. Phys. **B566**, 469 (2000) [arXiv:hep-ph/9907385].

[25] C. Anastasiou, T. Gehrmann, C. Oleari, E. Remiddi and J.B. Tausk, Nucl. Phys. **B580**, 577 (2000) [arXiv:hep-ph/0003261].

[26] T. Gehrmann and E. Remiddi, Nucl. Phys. **B580**, 485 (2000) [arXiv:hep-ph/9912329].

[27] C. Anastasiou, E.W.N. Glover and C. Oleari, Nucl. Phys. **B565**, 445 (2000) [arXiv:hep-ph/9907523]; Nucl. Phys. **B575**, 416 (2000) [arXiv:hep-ph/9912251].

[28] V.A. Smirnov, Phys. Lett. B **491**, 130 (2000) [arXiv:hep-ph/0007032];
T. Gehrmann and E. Remiddi, Nucl. Phys. B **601**, 248 (2001) [arXiv:hep-ph/0008287]; Nucl. Phys. B **601**, 287 (2001) [arXiv:hep-ph/0101124]; Comput. Phys. Commun. **141**, 296 (2001) [arXiv:hep-ph/0107173]; arXiv:hep-ph/0111255.

[29] L.W. Garland, T. Gehrmann, E.W.N. Glover, A. Koukoutsakis and E. Remiddi, arXiv:hep-ph/0112081.

[30] S. Catani, M.H. Seymour and Z. Trócsányi, Phys. Rev. **D55**, 6819 (1997) [arXiv:hep-ph/9610553].

[31] I. Antoniadis, C. Kounnas and K. Tamvakis, Phys. Lett. B **119**, 377 (1982).

[32] S.P. Martin and M.T. Vaughn, Phys. Lett. B **318**, 331 (1993) [arXiv:hep-ph/9308222].

[33] O.V. Tarasov, A.A. Vladimirov and A.Y. Zharkov, Phys. Lett. B **93**, 429 (1980);
S.A. Larin and J.A.M. Vermaseren, Phys. Lett. B **303**, 334 (1993) [arXiv:hep-ph/9302208].

[34] Z. Bern, in *Proceedings of Theoretical Advanced Study Institute in High Energy Physics (TASI 92)*, eds. J. Harvey and J. Polchinski, World Scientific, 1993 [arXiv:hep-ph/9304249].

[35] Z. Bern, L.J. Dixon, D.C. Dunbar and D.A. Kosower, Nucl. Phys. **B425**, 217 (1994) [arXiv:hep-ph/9403226];
Nucl. Phys. **B435**, 59 (1995) [arXiv:hep-ph/9409265].

[36] S. Ferrara and B. Zumino, Nucl. Phys. B **79**, 413 (1974);
M.F. Sohnius, Phys. Rept. **128**, 39 (1985);
A. Bilal, arXiv:hep-th/0101055.

[37] J. Wess and J. Bagger, *Supersymmetry and Supergravity*, second edition, Princeton Univ. Press, 1992 (Princeton Series in Physics).

[38] S.J. Gates, Jr., M.T. Grisaru, M. Rocek and W. Siegel, *Superspace: or one thousand and one lessons in supersymmetry*, Benjamin/Cummings, 1983 (Frontiers in Physics, 58).

[39] Z. Bern, L.J. Dixon and D.A. Kosower, Phys. Rev. Lett. **70**, 2677 (1993) [arXiv:hep-ph/9302280];
Z. Kunszt, A. Signer and Z. Trócsányi, Phys. Lett. B **336**, 529 (1994) [arXiv:hep-ph/9405386];
Z. Bern, L.J. Dixon and D.A. Kosower, Nucl. Phys. B **437**, 259 (1995) [arXiv:hep-ph/9409393].

[40] Z. Bern, L.J. Dixon and D.A. Kosower, Nucl. Phys. **B513**, 3 (1998) [arXiv:hep-ph/9708239].

[41] Z. Bern and A.G. Morgan, Nucl. Phys. **B467**, 479 (1996) [arXiv:hep-ph/9511336].

[42] Z. Bern, L.J. Dixon, M. Perelstein and J.S. Rozowsky, Phys. Lett. **B444**, 273 (1998) [arXiv:hep-th/9809160]; Nucl. Phys. **B546**, 423 (1999) [arXiv:hep-th/9811140].

[43] Z. Bern, L.J. Dixon, D.C. Dunbar, M. Perelstein and J.S. Rozowsky, Nucl. Phys. **B530**, 401 (1998) [arXiv:hep-th/9802162].

[44] L.D. Landau, Nucl. Phys. **13**, 181 (1959);
S. Mandelstam, Phys. Rev. **112**, 1344 (1958), **115**, 1741 (1959);
R.E. Cutkosky, J. Math. Phys. **1**, 429 (1960).

[45] J.E. Paton and H. Chan, Nucl. Phys. B **10**, 516 (1969);
P. Cvitanović, P.G. Lauwers and P.N. Scharbach, Nucl. Phys. B **186**, 165 (1981);
M. Mangano, S. Parke and Z. Xu, Nucl. Phys. B **298**, 653 (1988);
M. Mangano, Nucl. Phys. B **309**, 461 (1988).

[46] Z. Bern and D.A. Kosower, Nucl. Phys. B **362**, 389 (1991).

[47] V. Del Duca, L.J. Dixon and F. Maltoni, Nucl. Phys. B **571**, 51 (2000) [arXiv:hep-ph/9910563].

[48] G. Mahlon, Phys. Rev. **D49**, 4438 (1994) [arXiv:hep-ph/9312276]; Z. Bern, G. Chalmers, L.J. Dixon and D.A. Kosower, Phys. Rev. Lett. **72**, 2134 (1994) [arXiv:hep-ph/9312333]; Z. Bern, L.J. Dixon, D.C. Dunbar and D.A. Kosower, Phys. Lett. B **394**, 105 (1997) [arXiv:hep-th/9611127].

[49] L. Lewin, *Dilogarithms and Associated Functions*, Macdonald, 1958.

[50] S. Catani, Phys. Lett. **B427**, 161 (1998) [arXiv:hep-ph/9802439].

[51] B.S. DeWitt, Phys. Rev. **162**, 1195 (1967); G. 't Hooft, in *Acta Universitatis Wratislavensis no. 38*, 12th Winter School of Theoretical Physics in Karpacz, *Functional and Probabilistic Methods in Quantum Field Theory*, Vol. 1 (1975); B.S. DeWitt, in *Quantum gravity II*, eds. C. Isham, R. Penrose and D. Sciama, Oxford, 1981.

[52] L.F. Abbott, Nucl. Phys. B **185**, 189 (1981).

[53] L.F. Abbott, M.T. Grisaru and R.K. Schaefer, Nucl. Phys. B **229**, 372 (1983).

[54] A.G. Pickering, J.A. Gracey and D.R.T. Jones, Phys. Lett. B **510**, 347 (2001) [Phys. Lett. B **512**, 230 (2001)] [arXiv:hep-ph/0104247].

[55] K.G. Chetyrkin and A. Retey, arXiv:hep-ph/0007088.

[56] P. Boucaud, J.P. Leroy, J. Micheli, O. Pene and C. Roiesnel, JHEP **9812**, 004 (1998) [arXiv:hep-ph/9810437]; K.G. Chetyrkin and T. Seidensticker, Phys. Lett. B **495**, 74 (2000) [arXiv:hep-ph/0008094].

[57] M. Lüscher and P. Weisz, Nucl. Phys. B **452**, 234 (1995) [arXiv:hep-lat/9505011]; C. Christou, A. Feo, H. Panagopoulos and E. Vicari, Nucl. Phys. B **525**, 387 (1998) [arXiv:hep-lat/9801007], err. *ibid.* **B608**, 479 (2001); A. Bode and H. Panagopoulos, Nucl. Phys. B **625**, 198 (2002) [arXiv:hep-lat/0110211].

[58] D.J. Gross and F. Wilczek, Phys. Rev. Lett. **30**, 1343 (1973); H.D. Politzer, Phys. Rev. Lett. **30**, 1346 (1973).

[59] W.E. Caswell, Phys. Rev. Lett. **33**, 244 (1974); D.R.T. Jones, Nucl. Phys. B **75**, 531 (1974); E.S. Egorian and O.V. Tarasov, Theor. Math. Phys. **41**, 863 (1979) [Teor. Mat. Fiz. **41**, 26 (1979)].

[60] L.V. Avdeev and O.V. Tarasov, Phys. Lett. B **112**, 356 (1982).